coatings

Systematic Review

Antimicrobial Activity of Photocatalytic Coatings on Surfaces: A Systematic Review and Meta-Analysis

Francesca Ubaldi, Federica Valeriani *, Veronica Volpini, Giusy Lofrano and Vincenzo Romano Spica

Department of Movement, Health and Human Sciences, University of Rome "Foro Italico", 00135 Rome, Italy; f.ubaldi@studenti.uniroma4.it (F.U.); v.volpini@studenti.uniroma4.it (V.V.); giusy.lofrano@uniroma4.it (G.L.); vincenzo.romanospica@uniroma4.it (V.R.S.)

* Correspondence: federica.valeriani@uniroma4.it

Abstract: Photocatalytic technologies represent an innovative method to reduce microbial load on surfaces, even considering recent public health emergencies involving coronaviruses and other microorganisms, whose presence has been detected on surfaces. In this review paper, the antimicrobial efficacy of various photocatalysts applied by different coating methods on different surfaces has been compared and critically discussed. Publications reviewing the use of photocatalytic coatings on surfaces for antimicrobial effectiveness have been examined. Clear search parameters were employed to analyze the PubMed, Scopus, and WOS databases, resulting in 45 papers published between 2006 to 2023 that met the inclusion criteria. The paper assessed various types of photocatalytic coatings that targeted different microbial objectives. Based on the pooled data analysis, the TiO_2 coating exhibited a substantial effect in decreasing bacteria strains, both Gram-positive and -negative (99.4%). Although the diversity of these technologies poses significant obstacles to obtaining a comprehensive final assessment of their effectiveness and feasibility for surface application, subgroup analysis indicated significant variations in the removal efficiency of Gram-positive strains based on different surface types ($p = 0.005$) and time of exposure ($p = 0.05$). Photocatalytic coatings provide a promising approach to combating the spread of microorganisms on surfaces. Further "in-field" investigations are necessary in the foreseeable future to explore and optimize this novel and exciting health technology.

Keywords: photocatalysts; surfaces; coatings; disinfection; nanotechnologies

check for updates

Citation: Ubaldi, F.; Valeriani, F.; Volpini, V.; Lofrano, G.; Romano Spica, V. Antimicrobial Activity of Photocatalytic Coatings on Surfaces: A Systematic Review and Meta-Analysis. *Coatings* **2024**, *14*, 92. https://doi.org/10.3390/coatings14010092

Academic Editors: Tsvetelina Batsalova and Denitsa Kiradzhiyska

Received: 8 December 2023
Revised: 4 January 2024
Accepted: 8 January 2024
Published: 10 January 2024

1. Introduction

Ensuring human health is the primary challenge of the twenty-first century. The COVID-19 pandemic has brought to light how health threats can spread rapidly on a global scale. One of the ways infectious diseases can spread is through "indirect contact" or "fomite" exposure. Contaminated surfaces have the potential to transfer pathogens to the mucous membranes of individuals, thereby making them more vulnerable to infections [1]. Indirect contact can play an important role in the spread of respiratory diseases [2–4]. More resistant pathogens have a higher likelihood of spreading through the air or staying on surfaces until they meet susceptible individuals [5]. The risk of transmission through indirect contact depends on various factors, including the surface type [6,7].

Traditional disinfection methods typically involve using chemicals, ultraviolet radiation (UV), or other physical treatments to reduce the microbial load and lower the infective dose. Nevertheless, some bacteria can form biofilms and become resistant to these disinfection methods, making it more challenging to eliminate them [8,9]. Biofilms are present in healthcare facilities and are not easily eliminated by disinfectants. Indeed, biofilms are a breeding ground for pathogens, including multi-drug resistant organisms, and they are linked to healthcare-associated infections (HAIs) [10]. Biofilms can form themselves to various surfaces such as metals, plastics, or tissues. Their growth on medical devices and implants, such as heart valves, pacemakers, vascular grafts, catheters, prosthetic joints, intrauterine devices, sutures, and contact lenses, is a significant concern because it can lead to infections. There are several types of biofilms in healthcare settings, including hydrated biofilms and dry surface biofilms, and these cannot be treated in the same way. The inability to find an adequate technique significantly increases the disease burden on patients and healthcare systems. Thus, it is essential to advance innovative methods to combat the expansion of biofilms [11].

Several technologies, such as hydrogen peroxide steam, UV light, and heavy metal-coated surfaces (copper and silver), have been proven to be effective for disinfecting environmental surfaces. Researchers have been investigating designing surfaces with bactericidal or bacteriostatic activities for several years [12]. Various strategies have been used to combat pathogens, including surface coatings with antibiotics, biocides, metals, enzymes, and organic compounds [13]. The use of photocatalysts to coat surfaces, bestowing antimicrobial properties, is becoming increasingly useful. During the photocatalysis process, the interaction of light with semiconductors results in the formation of highly reactive oxygen species (ROS) such as hydrogen peroxide, singlet oxygen, superoxide radical anions, and hydroxyl radicals [14–17]. During this process, ROS act as antimicrobial agents, causing serious damage to nucleic acids, lipids, and proteins and inhibiting or exterminating microorganisms and pathogens. The field of nanobiotechnology has advanced significantly in recent years, allowing for the synthesis of nanomaterials with specific shapes and sizes. This has greatly improved the effectiveness of antimicrobial materials. Nanoparticles are particularly effective for antibacterial activity due to their unique chemical and physical properties, large surface areas, high heat stability and resistance, and broad-spectrum antibacterial activities [14,15]. Current research is concentrating on developing nanostructured surfaces for disinfection using photocatalytic materials and visible light. Recently, new strategies were proposed to overcome the limits of photocatalysts, such as the need to use high-energy UV light, looking toward using visible light-driven photocatalysts [18–20]. The ideal material or coating should be activated under artificial light conditions, especially considering the application in a hospital setting [18–22].

Based on the typologies of the coating process, the antimicrobial surfaces can be classified as passive, reducing the adhesion of microorganisms, or active, killing microorganisms upon contact. Passive or active surfaces can have several proprieties such as super-wettability, super-hydrophobicity, superoleophobicity, and omniphobicity [21]. Several technologies have been achieved to immobilize photocatalysts onto surfaces [22]. The synthesis of nanostructured materials can be realized by approaches such as sol-gel routes, hydrothermal and solvothermal methods, vapor- or plasma-assisted methods, or deposition of pre-synthesized nanostructured materials exploiting a wet-chemical process such as impregnation, dip, or spin coating. Each synthesis process can have advantages and disadvantages, and recent reviews have underlined, through a descriptive approach, the several applications to contrast microbial loads and future thoughts in hospital settings through descriptive approaches [23–26].

The purpose of the present systematic review and meta-analysis was to explore the antimicrobial effectiveness of several photocatalytic coatings on different surfaces, analyzing the data coming from the available literature on this topic through a quantitative approach and showing perspectives for the future.

2. Materials and Methods

2.1. Study Design and Strategy of Search

The Preferred Reporting Items for Systematic Review and Meta-Analysis (PRISMA) guidelines were used to identify eligible articles to explore the antimicrobial effectiveness of photocatalytic coatings on surfaces [27]. The search strategy has been registered in PROSPERO (reference number CRD42023449501).

Relevant literature on this theme was collected through a systematic search of three electronic databases (PubMed, Scopus and Web of Science) that were interrogated using the following terms: ("(antimicrobial or antibacterial)" AND "surfaces" AND "photocatalysis" AND "coating"). A search was conducted on three databases using different search criteria such as title, abstract, MeSH terms, and keywords. The period considered for the article collection was extensive to obtain a total overview of the topic (from June 2000 to 31 July 2023). The reference lists of each article were also checked to find additional relevant citations.

2.2. Inclusion and Exclusion Criteria

This review only considered studies that were based on the English language; analytic study designs; and "in vivo", "in vitro", and "in field" studies. Studies such as clinical trials, reviews, meta-analyses, case studies, case reports, proceedings, qualitative studies, editorials, commentary studies, studies without a control group, studies with incomplete designs (such as ecological studies), and any other types of study were excluded from the database. Extracted data from the three databases, such as titles and abstracts, were transferred to the site Covidence—Better systematic review management [28] for the relevance assessment process. The process of selecting studies involved a several-step exclusion process, involving four reviewers who independently investigated the titles and abstracts of the studies. During this multi-step exclusion process, reviewer consensus was obtained. Titles and abstracts acquired from the three databases were transferred to the reference site Covidence—Better systematic review management for the relevance assessment process. The next step was screening by title and abstracts the potentially eligible studies, following the inclusion criteria stated above; the screening was conducted by 4 authors (F.V., F.U., V.V., and G.L.) independently. Then, full texts were read independently by the 4 authors (F.V., F.U., V.V., and G.L.) with a later discussion about their inclusion in the review. Disagreements were achieved by consensus among the authors. We included articles from the inception to July 2023. The review process is represented in Figure 1 (PRISMA flow diagram of the systematic review process).

2.3. Data Synthesis

We used Comprehensive Meta-Analysis (CMA) software v.4 (Biostat Inc., Englewood, NJ, USA) to combine data. Our goal was to compare the effectiveness of a functionalized surface coated with TiO_2 against different bacterial strains (negative and positive Gram strains). To do this, we collected information on the rate of bacterial reduction, the wavelength of the light source, the time of exposure, the type of surfaces, and the method of coating. We calculated the eradication rates in both the case and control groups, as well as any side effects, and reported them as an event rate. The 95% confidence interval (95% CI) was also calculated. Hedges' g standardized mean difference statistic was used to calculate fixed and random effects model estimates. To evaluate statistically significant heterogeneity, we used the I_2 (percentage of variation reflecting true heterogeneity), τ_2 (random-effects between study variance), and p-value from Cochran's Q test. When there was good homogeneity amongst the studies included ($I_2 < 50\%$, $p > 0.1$), we employed the fixed effects model. Conversely, the random effects model was used in cases where the studies included shown significant heterogeneity ($I_2 \geq 50\%$, $p \leq 0.1$). To perform a sensitivity analysis, the effects model was altered, or individual studies were excluded. Funnel plots were also utilized to explore potential publication bias. Meta-regression and subgroup analyses were performed to explore the sources of heterogeneity expected [29–31]. For meta-regression analysis, the wavelength, the time of exposition, the type of surfaces, and the method of coating of the studies were considered.

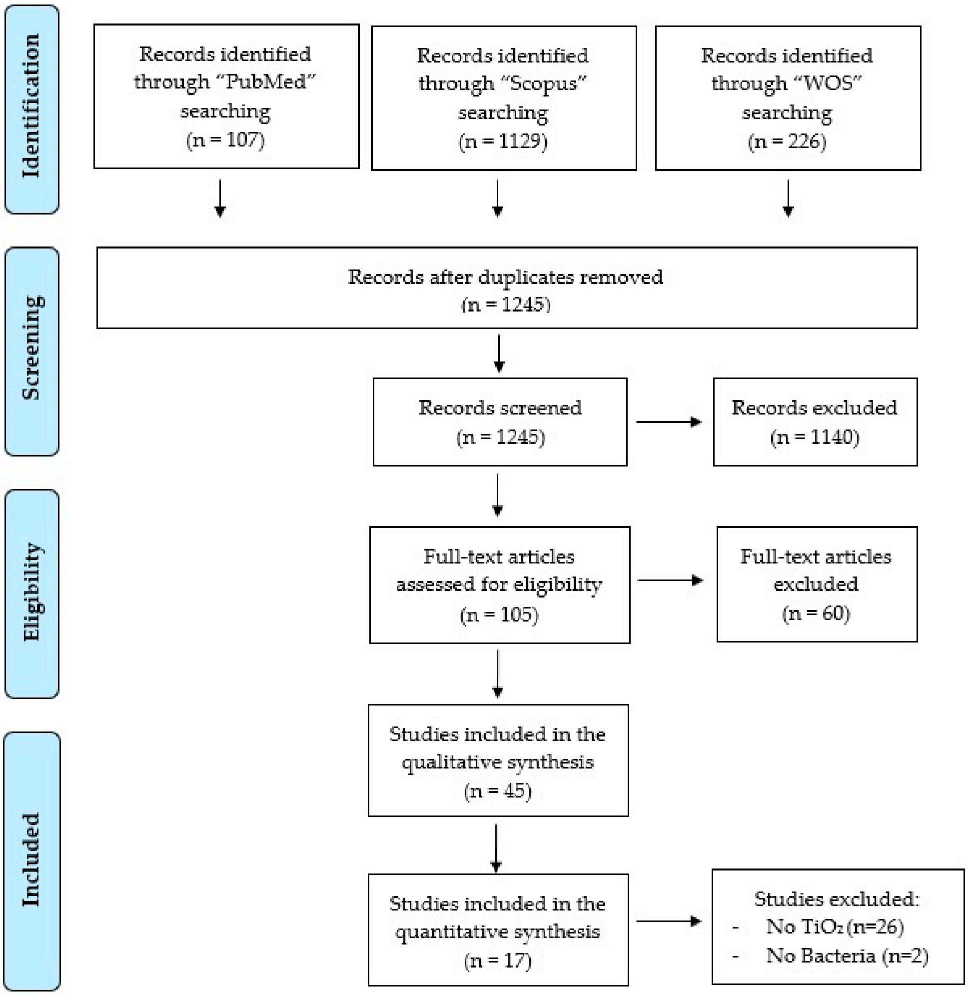

Figure 1. PRISMA flow diagram of the systematic review process.

3. Results and Discussion

3.1. Articles Selection

There has been a growing interest in using photocatalytic coatings to eliminate microorganisms, and this is well-reflected in scientific literature. Research related to the combination of "antimicrobial or antibacterial" properties, "surfaces", "photocatalysis", and "coatings" has increased exponentially in recent decades, as can be seen in Figure 2A. Additionally, bibliometric analysis of the literature shows that a significant number of researchers are actively studying this subject in more countries around the world (Figure 2B).

It is important to note that regions with lower research activity on this issue overlap with those that should prioritize antimicrobial resistance surveillance, such as Sub-Saharan Africa [32].

A total of 1462 records were found, and, after screening, 1245 were included, and 105 were assessed for eligibility. In total, 5 papers were excluded because they did not include any control group, 24 articles because they considered textile surfaces, 5 articles did not use any light source, and 26 articles because they were not pertinent. Finally, 45 articles met the inclusion criteria and were included in the qualitative synthesis [33–77]. For each article, the following data were reported: author, year, country, type of surface, type of photocatalyst, dose of photocatalyst, type of coating method, details of coating method, and main results (Table 1); author, year, country, microbial target, initial CFU (Colony Forming Units), microbial reduction, light source, wavelength of light, distance of light source from surface, characteristics of light source, time of light exposition, and test for evaluation of antimicrobial activity (Table 2).

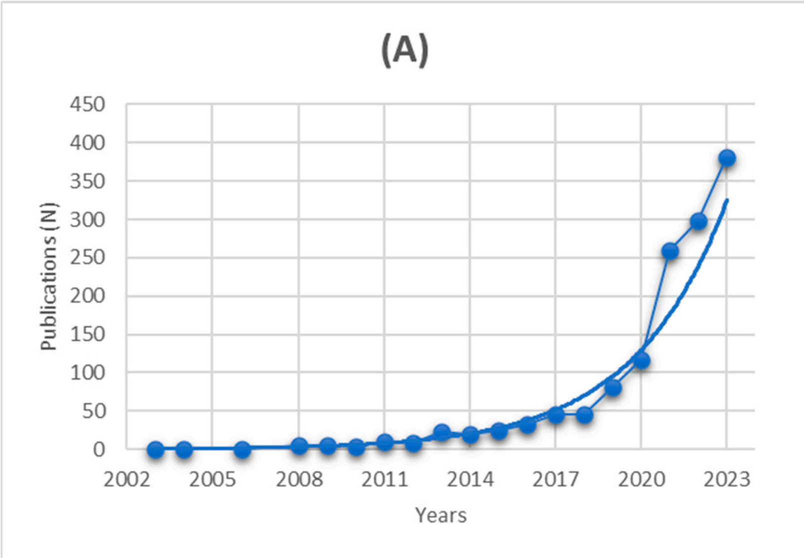

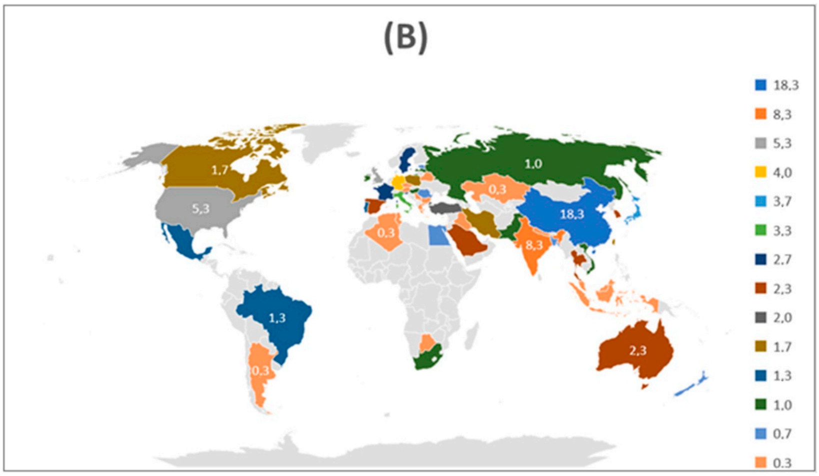

Figure 2. Graphics reporting the bibliometric analysis of literature. (**A**) The trend in the number of publications per year in the total of 1462 records found (date of search: from the inception to databases and July 2023) using the following combinations of topic keywords: "antimicrobial or antibacterial" properties, "surfaces", "photocatalysis", and "coatings". (**B**) The percentage of distribution of research in the countries of the world (using Bing Technologies and sources of data: Australian Bureau of Statistics, GeoNames, Geospatial Data Edit, Microsoft, Naviinfo, Open Places, OpenStreetMap, TomTom, Wikipedia, and Zenrin).

Table 1. A summary of the key findings and main features of the studies that were included in the systematic review.

Author, Year, Country	Type of Surface	Type of Photocatalyst	Dose of Photocatalyst	Type of Coating Method	Details of Coating Method	Main Results	Reference
Akgun et al., 2011, Turkey	Glass	Ag-TiO_2	6 mL of $Ti[O(CH_2)_3CH_3]_4$; 0.2 g $AgNO_3$	Spin coating	The cleaned substrate was coated with Ag-TiO_2 using a spin coater at 2300 rpm for 30 s. The coating process was repeated three times, and the resulting films were dried at 100 °C for 1 h. Subsequently, the films were calcined in air at 250 °C, 450 °C, and 650 °C for 6 h and then cooled to room temperature.	Under any given illumination condition, the Ag-doped films had increased bactericidal and photocatalytic activity compared to TiO_2 thin films.	[47]

Table 1. *Cont.*

Author, Year, Country	Type of Surface	Type of Photocatalyst	Dose of Photocatalyst	Type of Coating Method	Details of Coating Method	Main Results	Reference
Álvarez et al., 2022, Spain	Glass	TiO_2	NA	NA	Glass pre-exposed to UVA for 4 h, placed in a sterile dish. HCoV-229E was applied dropwise to the surface and covered with transparent PVC film.	The TiO_2-coated glass inactivates coronaviruses in a time-dependent manner on contact under daylight illumination.	[73]
Barthomeuf et al., 2019, France	Glass	TiO_2	NA	Sputtering deposition	A glass substrate was loaded into the deposition chamber after pre-sputtering the target in pure argon (Ar) for 10 min. Then, a mixture of argon (Ar) and oxygen (O_2) gas was injected into the sputtering chamber.	After photoactivation with UVA radiation for 20 min, TiO_2 coatings had a strong bactericidal effect.	[66]
Bletsa et al., 2023, Sweden	Glass	Ag/TiO_x	NA	Spin coating	The substrate holder was placed 20 cm above the burner for 15 s to deposit nanoparticles. The flame annealing process was conducted 20 cm above the burner using a xylene flame under cooling conditions. Stabilization was achieved by spin-coating at 100–500 rpm for 10 s and at 1000–4000 rpm for 50 s.	The compound was photocatalytically active with the visible light exposition.	[34]
Bonetta et al., 2013, Italy	Ceramics	TiO_2	1 mg cm^2	Chemical process	No details.	Bacterial concentration was reduced for all the microbes exposed to UV irradiation.	[50]
Chawengkijwanich et al., 2008, Thailand	Polypropylene	TiO_2	NA	Manual coating	TiO_2 was manually coated onto one side of the oriented polypropylene (OPP) film using a bar coater at room temperature.	There was a synergetic effect of TiO_2-coated packaging film with UVA light.	[40]
Chien et al., 2012, Vietnam	Ceramic	SiO_2/TiO_2	NA	Dip coating	Films were dip-coated onto ceramic tile substrates and annealed on a hot plate at 300 °C for 5 min, after which the substrates were calcined at 500 °C for 2 h. This process was repeated three times.	The films had high antibacterial activity by removing *E. coli*.	[48]
Chuang et al., 2017, Taiwan	Glass	ZnO/Ag_2O	NA	Sputtering deposition	Deposition was carried out using an RF magnetron sputtering system with a gas flow rate of 40 sccm. The sputtering times were 5 min (Ag_2O) and 30 min (ZnO/Ag_2O), with a power of 30 W and a working pressure of 2×10^{-3} torr at room temperature.	Ag_2O also has a great ability to kill bacteria, which may be due to the release of Ag^+ ions and the formation of photoelectrons and holes to generate active species to destroy bacteria.	[58]

Table 1. *Cont.*

Author, Year, Country	Type of Surface	Type of Photocatalyst	Dose of Photocatalyst	Type of Coating Method	Details of Coating Method	Main Results	Reference
Clemente et al., 2019, UK	Glass	TiO_2	0.5 ± 0.05 mg	Dip coating	Slides were fixed to a motor-driven bar, which allowed an immersion and withdrawal rate of 3 cm min^{-1}. Then, they were immersed in the TiO_2 suspension.	There were increased intracellular levels of oxidative stress, which over 24 h were lethal for *S. aureus*.	[67]
Cuadra et al., 2023, Spain	Glass	TiO_2-Ag	2.6 mL of titanium (IV) bis (acetylacetonate) diisopropoxide (75 wt % in isopropanol)	Sputtering deposition; spray coating	Titanium (IV) bis(acetylacetonate) diisopropoxide and EtOH were mixed for 30 min. The solution was applied to a soda-lime glass substrate heated to 450 °C and then heated to 550 °C on a hot plate.	The films had strong antibacterial activities after irradiation under UV-light for 4 h.	[35]
Deng et al., 2016, China	Poly vinyl chloride (PVC)	I-TiO_2	200 mL TiO_2 sol, 5 mL HI	Dip coating	PVA was dissolved in boiling water, then cooled. PVC pieces were dipped in the solution and removed. Then, the PVC pieces were immersed in I-TiO_2 solution to obtain I-TiO_2/PVC.	I-TiO_2/PVC had an excellent photocatalytic antibacterial activity, which can limit the propagation of the *E. coli*	[56]
Du et al., 2022, China	Polyure thane	Photocatalytic conductor polymer (PTET-T-COOH)	14 mg	Drop coating	4,4′-Diphenylmethane diisocyanate (MDI) and polycarbonate diol (PCDL) were each placed in a vacuum dryer at 80 °C for 30 min to melt prior to the reaction. After stirring the liquid mixture for 1 h at 80 °C, the pre-polyurethane was ready. 1,4-Butanediol was added to the pre-polyurethane and stirred for 30 min at 80 °C, and the polyurethane (PU) was prepared. The mixture was dropped onto a glass slide.	Under visible light irradiation, (PTET-T-COOH)-PU coating demonstrated an inactivation of *S. epidermidis* concentration in 6 h.	[74]
Dunnill et al., 2009, UK	Glass	N-doped TiO_2	NA	Atmospheric pressure chemical vapor deposition (APCVD)	Depositions were performed on SiO_2-coated glass slides after cleaning with water, acetone, petroleum ether, and propan-2-ol. The slides were then placed in an APCVD reactor and heated from room temperature to 500 °C at a rate of 10 °C/min.	The compound killed 99.9% of an *E. coli* suspension containing more than 10^4 viable bacteria, when exposed under white light for 24 h.	[43]
Evans et al., 2007, UK	Stainless steel	TiO_2	NA	Flame-assisted CVD (FACVD) (for silica); atmospheric pressure chemical vapor deposition (APCVD) (for titania)	The titania deposition was carried out using a horizontal cold wall APCVD quartz reactor, and precursors were supplied via bubblers. The steel substrates were cleaned with warm water and detergent before air drying. The silicon dioxide films were grown in a FACVD reactor.	The TiO_2 film is bio-active and that the timescale for 100% kill (6 log reduction) was between 120 and 180 min.	[38]

Table 1. *Cont.*

Author, Year, Country	Type of Surface	Type of Photocatalyst	Dose of Photocatalyst	Type of Coating Method	Details of Coating Method	Main Results	Reference
Fu et al., 2023, Israel	Glass	nAg/nTiO_2	NA	Dip coating; Spray coating	The glass substrate was dipped into TiO_2 gel four times, air-dried for 5 min between each immersion, and then calcined. An airbrush was used to spray TiO_2 suspension above the glass substrate, which was then calcined for 2 h at 200 °C.	The nAg/nTiO_2-coated sample reached 5.36 log virus reduction after 90 min under light source.	[36]
Guo et al., 2013, China	Glass	TiO_2	79.87 g/mol	Dip coating	The substrate was dip-coated with a TiO_2 film. The TiO_2 suspension was prepared from ethanol and glycerol. Then, it was stirred for 15 min, before the substrate was dipped into it (for 5 min). TiO_2-coated glass was calcinated at 450 °C for 120 min.	There was a total inactivation of *E. coli* within a relatively short time.	[51]
Hossain et al., 2018, Bangladesh	Glass	Fe-doped TiO_2–MWCNT (multiwalled carbon nanotubes)	NA	Drop coating	Soda lime silica glass was rinsed with alcohol and distilled water, then dried at 100 °C. TiO_2 gel films were obtained by coating a precursor solution onto the glass. The coated substrates were pretreated and annealed for 20 min at 200 °C. The coating process was repeated two times, followed by annealing at 500 °C for 2 h.	The nanocomposite could be used as an effective growth inhibitor of *E. coli*.	[63]
Jalvo et al., 2017, Spain	Glass	TiO_2	2 mL	Smearing (glass slides); impregnation (glass filters)	TiO_2 suspension applied to glass slides by smearing and to glass filters by impregnation. Substrates were dried at 110 °C before and after deposition and weighed to evaluate photocatalyst.	There was an antibacterial effect due to extensive membrane damage and significant production of ROS.	[59]
Jalvo et al., 2018, Spain	Glass	TiO_2	16.5 mL	Spray coating	Electrosprayed drops were deposited on round glass coverslips, attached to a flat collector that was horizontally arranged.	Light exposition caused membrane damage, with no cell regrowth.	[64]
Krumdieck et al., 2019, New Zealand	Steel	TiO_2	NA	Pulsed-pressure metalorganic chemical vapor deposition (pp-MOCVD)	Steel substrates were cleaned by abrading followed by ultrasonication in a silicon-free detergent/water solution, rinsed, and dried prior to loading into the pp-MOCVD chamber for a 30 min bake.	The pp-MOCVD approach could represent a strategy to support catalysts.	[68]
Leyland et al., 2016, Ireland	Glass	F, Cu-doped TiO_2	NA	Dip coating	Substrates were immersed in sol and then drawn vertically. The coated glass was dried and heated at 550 °C for 90 min.	There was a bacterial reduction of $\log_{10} = 4.2$ (visible light) and $\log_{10} = 1.8$ in darkness.	[57]

Table 1. *Cont.*

Author, Year, Country	Type of Surface	Type of Photocatalyst	Dose of Photocatalyst	Type of Coating Method	Details of Coating Method	Main Results	Reference
Li et al., 2022, Singapore	Polyurea	La-, Ce-, Pr-, and Gd (RE-dopants)-doped nano-ZnO	NA	NA	All chemicals were heated and placed in the mixer for 180 s. Then, the polyurea was poured into Teflon molds and placed in an oven at 70 °C to cure for 48 h.	These polyurea coatings had a high bactericidal rate over 85%.	[75]
Lin et al., 2008, China	Poly vinyl chloride (PVC)	TiO_2	NA	Dip coating	The PVC sheets were immersed in the precursor suspension (THF) and then pulled out at a speed of 1200 mm/h and dried in air for 1 h.	The pre-irradiated TiO_2/PVC had an excellent antibacterial adhesion and sterilization activity.	[41]
Muranyi et al., 2010, Germany	Glass	TiO_2	NA	Dip coating	Sol was made by controlled hydrolysis and condensation. Ethanol was split into two beakers. Part A had water and nitric acid, and Part B had TPOT. Part A was slowly added to Part B while stirring with a magnetic stirrer for 30 min.	The titanium dioxide layers can very effectively decompose *K. rhizophila* cells.	[45]
Nandakumar et al., 2017, USA	Ceramics	TiO_2	NA	Multiple coating	The dispersions were applied as uniform coatings on ceramic tiles. A second coat of anatase was applied after the tiles were dried. Coatings of silica were similarly prepared.	The *S. aureus* reduction under visible light gradually decreased with increasing cut off limits up to 550 nm.	[60]
Oder et al., 2020, Slovenia	Polysty rene	Cu-TiO_2	400 mg of the $H_2Ti_3O_7$ nanotube; 100 mL of 0.5 mM solution of Cu^{2+}	Smearing	Petri dishes were treated with compressed air and smeared evenly. After the deposition, they were rinsed with water and put in the oven at 60 °C overnight.	There is a short term microbiocidal effectiveness of TiO_2 nanotube coatings irradiated with UVA on *L. pneumophila*.	[70]
Page et al., 2007, UK	Glass	Ag-TiO_2	17.02 g Titanium n-butoxide; 0.8510 g silver nitrate	Dip coating	A dip-coating apparatus was used to eliminate the slide from the sol (speed of 120 cm min^{-1}).	Ag-doped titania coatings were more photocatalytically and antimicrobially active than a titania coating.	[39]
Pessoa et al., 2017, Brazil	Polyurethane; Poly-dimethyl-siloxane	TiO_2	NA	Atomic layer deposition (ALD)	ALD consisted of the different steps: 1. $TiCl_4$ pulse of 0.25 s; 2. purge of 2 s; 3. H_2O pulse of 0.25 s; 4. purge of 2 s. During the deposition, the base pressure of the reactor was lower than 10^{-2} mbar, and the working pressure was kept around of 1.0 mbar through the insertion of 300 sccm of N_2.	A reduction was observed in comparison to control.	[61]

Table 1. *Cont.*

Author, Year, Country	Type of Surface	Type of Photocatalyst	Dose of Photocatalyst	Type of Coating Method	Details of Coating Method	Main Results	Reference
Pezzoni et al., 2020, Argentina	Glass	TiO_2	NA	Spin coating	The films were prepared by spin-coating (3100 rpm for 30 s) on glass slides at 35 °C solution temperature and 30% relative humidity.	There was a high percentage of cell membrane disruption, compared to non-treated biofilms.	[71]
Roldán et al., 2014, Argentina	Glass	Ag-SiO_2/TiO_2	NA	Dip coating	SiO_2 and Ag-doped SiO_2 layers were deposited and heat-treated at 450 °C for 30 min. The TiO_2 coating was heat-treated at 450 °C for 1 h and all the slides were coated on both sides.	It was important that Ag NPs and TiO_2 are enclosed together because SiO_2/Ag–TiO_2 has a higher bactericidal effect than Ag–SiO_2/TiO_2.	[52]
Sayilkan et al., 2009, Turkey	Glass	TiO_2-Sn^{4+}	8.4 g (w/w = 10); 18.8 g (w/w = 20); 32.2 g (w/w = 30); 50.1 g (w/w = 40); 75.2 g (w/w = 50)	Spin coating	The glass surface was pre-coated with a solution consisting of 3-aminopropyltrimethoxy silane (AMMO), distilled water and isopropyl alcohol. Free hydroxyl groups, which are composed of hydrolysis of AMMO, behave as bridge between the film and the glass surface.	The films had higher antibacterial effect than undoped TiO_2.	[44]
Shieh et al., 2006, Taiwan	Glass; steel	TiO_2	NA	Sputtering deposition	Ar and O_2 were introduced to the RF sputter chamber. The substrate of sputter was loaded and after 120 s of deposition, the thickness of the TiO_x thin film was about 120 nm.	The coating technology can be applied effectively to surfaces with different degrees of roughness.	[33]
Szczawiński et al., 2011, Poland	Ceramics	TiO_2	NA	Sputtering deposition; atmospheric pressure chemical vapor deposition (APCVD); spray coating	Sputtering was performed in pure argon at a pressure of 4.4 Pa. TiO_2 targets of 100 mm diameter. For APCVD, titanium tetraisopropoxide (TTIP) was used as a precursor and stored in a glass Dreschler bubbler and maintained at 210 °C. Argon carrier gas was used to transport the TTIP through silicon and quartz lines to the vertical tube furnace. For spray coating, the same technique was used as for APCVD.	The strongest bactericidal effect of UV radiation was observed on the surfaces of tiles coated with TiO_2 by APCVD.	[46]
Tallósy et al., 2014, Hungary	Glass	Ag-TiO_2	0.6 mg/cm^2	Spray coating	No details.	There was an antibacterial effect against methicillin-resistant *S. aureus* under visible light.	[53]

Table 1. *Cont.*

Author, Year, Country	Type of Surface	Type of Photocatalyst	Dose of Photocatalyst	Type of Coating Method	Details of Coating Method	Main Results	Reference
Thongsuriwong et al., 2013, Thailand	Glass	ZnO	NA	Dip coating	ZnO thin films were deposited on soda lime glass substrates by the dip-coating method at a withdrawal speed of 1 cm/min at room temperature.	There was a complete inactivation of *E. coli* after 60 min of irradiation.	[49]
Todorova et al., 2023, Bulgaria	Glass	$PtSe_2$	NA	Sputtering deposition	The Pt pre-deposited glass substrates were placed in a three zone Chemical Vapor Deposition (CVD) reactor for the selenization procedure. Pt/glass samples were positioned in the thermal plateau of the central temperature zone (∼500 °C).	$PtSe_2$ coatings exhibited antibacterial behavior against *E. coli* in dark and UV irradiation conditions.	[37]
Valenzuela et al., 2019, Spain	Glass	ZnO	NA	Spray coating	The electrospray operated in a stable cone-jet mode at room temperature. The dry particles were deposited onto prewashed round glass coverslips attached to the collector. A bacterial suspension was loaded into a nebulizer, which generated an aerosol of 7 μL cm^{-2}, which was then applied on ZnO coated and uncoated glass surfaces.	There was >99.5% (2-log) of bacterial reduction.	[69]
Verdier et al., 2014, France	Glass	TiO_2	13.9 g/L	Drop coating	The cover-glasses were covered with coatings and placed under a sterile flow hood for air drying. Then, the semi-transparent coatings were sanded with fine sandpaper.	There was a difference in antibacterial activity between simple drop-deposited inoculum and inoculum spread under a plastic film.	[54]
Vihodceva et al., 2022, Latvia	Glass	Ag/AgCl/α-Fe_2O_3	0.200 g of $AgNO_3$; 0.200 mL of CH_2Cl_2; 0.400 g α-Fe_2O	Spin coating	Ethylene-vinyl acetate (EVA) polymer granules were dissolved in hexane by vigorous stirring at 40 °C temperature for 3 h. The suspension was deposited on cover glasses using the spin-coating technique (4000 rpm, 20 s). Then, the surfaces were heated at 40 °C for 2 h.	After 30 min of visible-light illumination, there was a >7-log reduction of *S. aureus*, even after 3 cycles of use.	[76]
Won et al., 2018, USA	Glass	Ag/TiO_2	NA	Dip coating	Glass substrate was etched in HCl for 30 min, rinsed, and dipped 10 times in TiO_2-ethanol solution that was prepared by suspending TiO_2 in ethanol for 20 min in sonicator.	N-Ag/anatase-TiO_2 <100 nm coated sample had the lowest post-UV bacterial attachment.	[65]

Table 1. *Cont.*

Author, Year, Country	Type of Surface	Type of Photocatalyst	Dose of Photocatalyst	Type of Coating Method	Details of Coating Method	Main Results	Reference
Xiao et al., 2014, China	Glass	Fe-doped TiO_2 with chitosan	0.05 g	Drop coating	Chitosan was dissolved in acetic acid, and then Fe-TiO_2 powder and Epichlorohydrin were added. Then, the suspension was spread on a slide glass, and the novel anti-fungal coating (ABAC) was prepared.	The ABAC is a promising antibacterial coating, useful for domestic, medical, and industrial applications.	[55]
Xu et al., 2022, China	Poly vinyl chloride (PVC)	Ag-decorated β-Bi_2O_3/$Bi_2O_{2.7}$	NA	Dip coating	The β-Bi_2O_3/$Bi_2O_{2.7}$ film was immersed horizontally in $AgNO_3$ solution for 30 min and then washed. The films were immersed horizontally in ascorbic acid solution for 20 min, and they were rinsed and dried at 60 °C in air.	The film was able to significantly reduce *E. coli* (>99.99%).	[77]
Yao et al., 2008, Japan	Silicone	Ag/TiO_2	NA	Dip coating	The catheters were dipped into an ethanol-ethyl acetate solution of modified silicone resin and into an ethanol–water solution of TiO_2 sol and silicon oxide compounds. After each dip-coating, the samples were heated and then cooled.	The coating could be useful and reusable as an antimicrobial coating for medical devices against nosocomial infections.	[42]
Yemmireddy et al., 2017, USA	Polyeth ylene	TiO_2	0.0625 mg/cm^2	Spray coating	Spray TiO_2 in ethanol on a steel surface. Put a plastic cutting board on the TiO_2-coated SS plate. Compress with Carver® press to transfer TiO_2 onto plastic cutting board.	Even after repeated use up to 5 times, the coating showed high durability and strong photocatalytic bactericidal properties.	[62]
Zhao et al., 2020, China	Titanium alloy rods (Ti-6Al-4V)	MoO_3-SiO_2-Ag_2O	NA	Sputtering deposition	Prior to the sputter deposition, the chamber was pumped down to a residual gas pressure of 5×10^{-4} Pa. The substrate samples were etched by Ar ion bombardment at a potential of −650 V for 20 min.	The coating had stronger bactericidal properties to Gram-negative and Gram-positive bacteria and fungi.	[72]

Table 2. Details of the microbial activity of the papers considered in the review.

Author, Year, Country	Microbial Target	Initial CFU (CFU/mL)	Microbial Reduction	Light Source	Wavelength of Light (nm)	Distance of Light Source from Surface (cm)	Characteristics of Light Source	Time of Light Exposition	Test for Evaluation of Antimicrobial Activity	Reference
Akgun et al., 2011, Turkey	*S. epidermidis*	NA	100%	UV	365	3	0.2 W/m^2	3 h; 6 h; 12 h	Disk diffusion assay; UV-induced bactericidal test; qualitative Ag ion release in bacteria inoculated agar media; surface topographical examination by laserscan profilometry	[47]
Álvarez et al., 2022, Spain	Human coronavirus 229E (*HCoV-229E*)	NA	99% of virus titer	D65 (radiation that emu-lates day-light)	380–750	25	1.8 W	234 min	Endpoint titration method	[73]
Barthomeuf et al., 2019, France	*L. monocytogenes*	10^8	2.5 log	UV	400	2	14 W/m^2	20 min	Plate counting	[66]
Bletsa et al., 2023, Sweden	*E. coli*; *S. aureus*; *P. aeruginosa*	10^8	1.4 log (*E. coli* after 15 min); 1.8 log (*E. coli* after 90 min); 1.2 (*P. aeruginosa* after 15 min); 2.7 (*P. aeruginosa* after 90 min); 1.3 (*S. aureus* after 15 min); 1.5 (*S. aureus* after 90 min)	Visible	400–600	NA	300 W	15 min; 30 min; 1 h; 90 min	Plate counting	[34]

Table 2. *Cont.*

Author, Year, Country	Microbial Target	Initial CFU (CFU/mL)	Microbial Reduction	Light Source	Wavelength of Light (nm)	Distance of Light Source from Surface (cm)	Characteristics of Light Source	Time of Light Exposition	Test for Evaluation of Antimicrobial Activity	Reference
Bonetta et al., 2013, Italy	*E. coli*; *S. aureus*; *P. putida*; *L. innocua*	10^4	*E. coli*: 1.5 log (180 min); *S. aureus*: 1 log (60 min); *P. putida*: 0.5 log (30 min); L. innocua: 0.5 log (20 min)	UV	350–380	10.3	9 W/m^2	20 min; 30 min 1 h, 180 min	Plate counting	[50]
Chawengkijwanich et al., 2008, Thailand	*E. coli*	10^7	3 log	UV	300–400	NA	20 W × 2 LED lamps	3 h	Plate counting	[40]
Chien et al., 2012, Vietnam	*E. coli*	10^9	70%	Visible	NA	NA	18 W	24 h	Plate counting	[48]
Chuang et al., 2017, Taiwan	*E. coli*; *S. aureus*	10^4	100%	Visible	NA	30	20 W	3 h	Plate counting	[58]
Clemente et al., 2019, UK	*S. aureus*	2.5×10^6	100%	UV	360	4	10 W/m^2	24 h	Plate counting	[67]
Cuadra et al., 2023, Spain	*E. coli*	4×10^5	93%	UV	NA	NA	0.5 W/m^2	4 h	Plate counting	[35]
Deng et al., 2016, China	*E. coli*	10^7	100%	Visible	420	NA	300 W	30 min	Plate counting	[56]
Du et al., 2022, China	*S. epidermidis*	10^8	100%	Visible	NA	NA	0.08 W/m^2	6 h	Plate counting	[74]
Dunnill et al., 2009, UK	*E. coli*	10^7	99,9%	UV	254	20	28 W	24 h (only the surface) + 24 h (surface + *E. coli*)	Plate counting	[43]
Evans et al., 2007, UK	*E. coli*	10^6	100%	UV	NA	NA	NA	3 h	Plate counting	[38]

Table 2. *Cont.*

Author, Year, Country	Microbial Target	Initial CFU (CFU/mL)	Microbial Reduction	Light Source	Wavelength of Light (nm)	Distance of Light Source from Surface (cm)	Characteristics of Light Source	Time of Light Exposition	Test for Evaluation of Antimicrobial Activity	Reference
Fu et al., 2023, Israel	*MS2 virus*	10^6	0.5 log reduction	UV	365	15	NA	90 min	Plate counting	[36]
Guo et al., 2013, China	*E. coli*	1×10^5	100%	UV	NA	NA	10 W/m^2	1 h	Plate counting	[51]
Hossain et al., 2018, Bangladesh	*E. coli*	NA	>80% (Fe-TiO_2); >90% (Ag-TiO_2)	Visible	NA	20	200 W	1 h	Plate counting	[63]
Jalvo et al., 2017, Spain	*S. aureus*; *P. putida*	NA	99.9%	UV	290–400	20	11.2 W/m^2	2 h	LIVE/DEAD Biofilm Viability Kit	[59]
Jalvo et al., 2018, Spain	*S. aureus*	10^8	99%	UV	NA	NA	11.2 W/m^2	18 h	LIVE/DEAD Biofilm Viability Kit	[64]
Krumdieck et al., 2019, New Zealand	*E. coli*	10^7	99.9% (UV); 3 log (visible)	UV	365	NA	NA	4 h	Plate counting	[68]
Leyland et al., 2016, Ireland	*S. aureus*	1×10^5	$\log_{10} = 4.2$	Visible	NA	NA	NA	24 h	Plate counting	[57]
Li et al., 2022, Singapore	*E. coli*; *P. aeruginosa*	NA	3.20 log mL^{-1} (*E. coli*); 3.92 log mL^{-1} (*P. aeruginosa*)	UV	NA	NA	NA	25 min	LIVE/DEAD Biofilm Viability Kit	[75]
Lin et al., 2008, China	*E. coli*	10^4	100%	UV	365	NA	8 W	90 min	Plate counting	[41]
Muranyi et al., 2010, Germany	*K. rhizophila*; spores of *A. niger* and *B. atrophaeus*	10^5	3 $\log_{10}$ (*k. rhizophila*), 0 (spores of *A. niger* and *B. atrophaeus*)	UVA	NA	NA	0.027 W/m^2	4 h	Plate counting	[45]

Table 2. *Cont.*

Author, Year, Country	Microbial Target	Initial CFU (CFU/mL)	Microbial Reduction	Light Source	Wavelength of Light (nm)	Distance of Light Source from Surface (cm)	Characteristics of Light Source	Time of Light Exposition	Test for Evaluation of Antimicrobial Activity	Reference
Nandakumar et al., 2017, USA	*S. aureus*	2×10^6	45%	UV; Visible	300–450	NA	1.8 W/m^2	18 h	Plate counting	[60]
Oder et al., 2020, Slovenia	*L. pneumophila*	300	90%	UV	365	23	15 W/m^2	24 h	Plate counting	[70]
Page et al., 2007, UK	*S. aureus*; *E. coli*; *B. cereus*	10^9 (*S. aureus*; *E. coli*); 10^8 (*B. cereus*)	99.9% (*S. aureus*; *B. cereus*), 69% (*E. coli*)	UV	365	NA	8 W	6 h	Plate counting	[39]
Pessoa et al., 2017, Brazil	*C. albicans*	10^6	70.4% (Polyurethane); 80% (Polydimethylsiloxane)	UV	365	NA	10 W/m^2	1 h	Plate counting	[61]
Pezzoni et al., 2020, Argentina	*P. aeruginosa*	NA	99.9%	UV	365	NA	18 W	3 h	Plate counting; membrane integrity evaluation	[71]
Roldán et al., 2014, Argentina	*E. coli*; *L. monocytogenes*; spores of *B. anthracis* and *C. perfringens*	1×10^6 (*E. coli*; *L. monocytogenes*); 1×10^9 (*B. anthracis* and *C. perfringens*)	85%	UV	365	NA	6 W	45 min (*E. coli*; *L. monocytogenes*); 2 h (*B. anthracis* and *C. perfringens*)	LIVE/DEAD Biofilm Viability Kit	[52]

Table 2. *Cont.*

Author, Year, Country	Microbial Target	Initial CFU (CFU/mL)	Microbial Reduction	Light Source	Wavelength of Light (nm)	Distance of Light Source from Surface (cm)	Characteristics of Light Source	Time of Light Exposition	Test for Evaluation of Antimicrobial Activity	Reference
Sayilkan et al., 2009, Turkey	*E. coli*; *S. aureus*	10^7	*E. coli*: 58.8% (*w*/*w* = 10); 66% (*w*/*w* = 20); 95.1% (*w*/*w* = 30); 98.6% (*w*/*w* = 40); 99.9% (*w*/*w* = 50); *S. aureus*: 68.2% (*w*/*w* = 10); 78.3% (*w*/*w* = 20); 96.9% (*w*/*w* = 30); 99.9% (*w*/*w* = 40); 99.9% (*w*/*w* = 50).	UV (only the surface was irradiated)	NA	20	1100 W/m^2 (prior to bacterial treatment, the surface with TiO_2–Sn^{4+} was irradiated)	1 h (prior to bacterial treatment, the surface with TiO_2–Sn^{4+} was irradiated)	Plate counting	[44]
Shieh et al., 2006, Taiwan	*E. coli*	10^5	99.9%	Visible (steel); UV (glass)	NA	NA	15 W × 4 lamps	5 h	Plate counting	[33]
Szczawiński et al., 2011, Poland	*S. aureus*	2.5×10^8	5.48–7.17 log	UV	254	0,57	16 W × 4 lamps	120 s	Plate counting	[46]
Tallósy et al., 2014, Hungary	*S. aureus*	10^4	99.9%	Visible	405	NA	NA	2 h	Plate counting	[53]
Thongsuriwong et al., 2013, Thailand	*E. coli*	2.3×10^5	100%	UV	NA	NA	NA	1 h	Plate counting	[49]
Todorova et al., 2023, Bulgaria	*E. coli*	2×10^6	Bacteria viability 7.3% (Pt 8 s = thickness of 9 nm) and 1.2% (Pt 10 s = thickness of 12 nm)	UV	NA	NA	0.1 W/m^2	6 h	LIVE/DEAD Biofilm Viability Kit	[37]

Table 2. *Cont.*

Author, Year, Country	Microbial Target	Initial CFU (CFU/mL)	Microbial Reduction	Light Source	Wavelength of Light (nm)	Distance of Light Source from Surface (cm)	Characteristics of Light Source	Time of Light Exposition	Test for Evaluation of Antimicrobial Activity	Reference
Valenzuela et al., 2019, Spain	*S. aureus*	10^8	>99.5%	UV	365	20	27 ± 3 W/m^2	2 h	Plate counting; LIVE/DEAD Biofilm Viability Kit	[69]
Verdier et al., 2014, France	*E. coli*	10^8	-0.91 ± 0.14 log	UV	NA	NA	2.5 W/m^2	6 h	Plate counting	[54]
Vihodceva et al., 2022, Latvia	*S. aureus*	10^7	100%	Visible	NA	NA	20 W $\times$ 2 LED lamp	30 min	Plate counting	[76]
Won et al., 2018, USA	*E. coli*	10^8	80%	UV	NA	20	1000 W	45 min	LIVE/DEAD Biofilm Viability Kit	[65]
Xiao et al., 2014, China	*E. coli*; *C. albicans*; *A. niger*	9.6×10^4	99.9% (*E. coli*); 97% (*C. albicans*); 95% (*A. niger*)	Visible	NA	NA	100 W	2 h	Plate counting	[55]
Xu et al., 2022, China	*E. coli*	10^7	>99.9%	Visible	NA	NA	5 W	18 h	Plate counting	[77]
Yao et al., 2008, Japan	*E. coli*; *S. aureus*; *P. aeruginosa*	10^6	99%	UV	NA	NA	10 W/m^2	20 min (*E. coli*); 90 min (*S. aureus*); 1 h (*P. aeruginosa*)	Cell attachment method	[42]
Yemmireddy et al., 2017, USA	*E. coli*	10^7	5.71 log	UV	254	NA	5 ± 0.05 W/m^2	3 h	Plate counting	[62]
Zhao et al., 2020, China	*E. coli*; *S. typhimurium*; *S. aureus*; *C. albicans*	1×10^5	100% (*E. coli*; *S. typhimurium*; *S. aureus*); 95,5% (*C. albicans*)	Visible	NA	NA	NA	1 h	Plate counting	[72]

3.2. Characteristics of the Selected Studies

The 45 articles included in the systematic review were published between 2006 [33] and 2023 [34–37], showing a positive growth trend: one article was published in 2006 [33], two in 2007 [38,39], three in 2008 [40–42], two in 2009 [43,44], one in 2010 [45], two in 2011 [46,47], one in 2012 [48], three in 2013 [49–51], four in 2014 [52–55], two in 2016 [56,57], five in 2017 [58–62], three in 2018 [63–65], four in 2019 [66–69], three in 2020 [70–72], five in 2022 [73–77], and four in 2023 [34–37]. Research related to the antimicrobial properties of photocatalytic processes has exponentially increased over the last few decades. Identifying alternative technologies to traditional methods is a necessary challenge for human health and ecosystem protection. Furthermore, the awareness of co-infection about COVID-19 has compelled researchers to explore potential solutions. This section discusses methods that have been used to prevent the growth of bacteria and fungi or as antiviral agents, such as carbon-based nanomaterials [78–81]. It is worth noting that photocatalysis has proven to be highly effective in inactivating various microorganisms, even resulting in their complete decomposition [82–84]. The main application of photocatalysis is in the preparation of self-cleaning surfaces. Several in vitro studies have shown its potential effectiveness as a semiconductor active in matrices such as water, air, and surfaces against various microorganisms. Although it has been tested in hospital settings, further research is needed to determine its effectiveness in real-world scenarios [85–89]. Moreover, there has been a recent increase in interest in using photocatalysis for indoor air purification and water treatment but also for assembly of masks and clothes and medical purposes such as wound healing [90–92].

Research in this field shows a global dimension and the studies were achieved in different countries: seven trials were performed in China [41,51,55,56,72,74,77], five in Spain [35,59,64,69,73], four in UK [38,39,43,67], three in USA [60,62,65], two in France [54,66], two in Taiwan [33,50], two in Turkey [44,47], two in Thailand [40,49], two in Argentina [52,71], one in Ireland [57], one in Singapore [75], one in Slovenia [70], one in Vietnam [48], one in Bulgaria [37], one in Israel [36], one in Germany [45], one in Latvia [76], one in Sweden [34], one in Brazil [61], one in Italy [50], one in Hungary [53], one in New Zealand [68], one in Poland [46], one in Japan [42], and one in Bangladesh [63]. All the studies considered a particular type of surface, a microbial target and a photocatalyst. Furthermore, they all presented microbial reduction data and a test for the evaluation of antibacterial properties.

For each study included in the systematic review, several factors that affected the effectiveness of disinfection were extracted, such as type of surface and photocatalyst, dosage, the process of deposition techniques, type of microorganisms, light source, and time of exposure. This operational parameter could affect the efficiency of the photocatalytic disinfection process. As shown in Table 1, 28 articles considered glass surface [33–37,39,43–45,47,49,51–55,57–59,63–67,69,71,73,76], 4 ceramics [46,48,50,60], 3 steel [33,38,68], 3 polyvinyl chloride (PVC) [41,56,77], 2 polyurethane [61,74], 1 polyurea [75], 1 polystyrene [70], 1 polypropylene [40], 1 titanium alloy rods (Ti-6Al-4V) [72], 1 polyethylene [62], 1 polydimethylsiloxane [61], and 1 silicone [42].

Regarding photocatalysts, 19 articles considered TiO_2 [33,38,40,41,45,46,50,51,54,59–62,64,66–68,71,73], 8 Ag with TiO_2 [34–36,39,42,47,53,65], 2 ZnO [49,69], 1 SiO_2/TiO_2 [48], 1 ZnO/Ag_2O [58], 1 I-TiO_2 [56], 1 Photocatalytic conductor polymer (PTET-T-COOH) [74], 1 N-doped TiO_2 [43], 1 Fe-doped TiO_2–MWCNT (multiwalled carbon nanotubes) [63], 1 F, Cu-doped TiO_2 [57], 1 La-, Ce-, Pr-, and Gd (RE-dopants)-doped nano-ZnO [75], 1 Cu-TiO_2 [70], 1 Ag-SiO_2/TiO_2 [52], 1 TiO_2-Sn^{4+} [44], 1 $PtSe_2$ [37], 1 Ag/AgCl/α-Fe_2O_3 [76], 1 Fe-doped TiO_2 with chitosan [55], 1 Ag-decorated β-Bi2O_3/$Bi_2O_{2.7}$ [77], and 1 MoO_3-SiO_2-Ag_2O [72]. Among several materials tested, TiO_2 is the most suitable for use in photocatalytic processes compared to ZnO, CeO_2, SnO_2, ZrO_2, CdS, and others. TiO_2, also known as white pigment, is commonly used as an additive to building and coating materials due to its high photocatalytic activity, physical and chemical stability in the dark, non-toxicity, lack of corrosion, and low cost [24].

The photocatalyst's effectiveness depends on the rate of ROS production at the semiconductor surface, which is influenced by various factors. These factors include material morphologies, element doping, oxidant addition, high surface area, and high light intensity [93]. The surface morphology of the photocatalyst has a direct impact on the adsorption of contaminants, which is crucial for photo-mineralization. The structure and features of the substrate significantly impact the effectiveness of disinfection. A greater pore structure and rougher surface can enhance the loading capacity of photocatalytic materials, as well as the adsorption capacity and contact area of the photocatalyst [94]. In addition, the loose texture structure and light scattering performance have significantly increased the specific surface area and light absorption capacity [95]. Moreover, the other aspects affected the disinfection efficiency, such as the wettability of surfaces depending on the super-hydrophilic, super-hydrophobic, and super-amphiphilic properties of the materials [96].

The dosage of photocatalysts is a crucial factor in defining the efficiency of disinfection or microbial load inactivation. However, the dose of photocatalyst used was always not mentioned in all the works, and the quantity is very different in several experiment designs: 6 mL of Ti[O(CH_2)3CH_3]4; 0.2 g $AgNO_3$ [47]; 1 mg cm^{-2} [50]; 0.5 ± 0.05 mg [67], 2.6 mL of titanium (IV) bis(acetylacetonate) diisopropoxide (75 wt % in isopropanol) [35]; 200 mL TiO_2 sol, 5 mL HI [56]; 14 mg [74]; 79.87 g/mol [51]; 2 mL [59], 16.5 mL [64]; 400 mg of the $H_2Ti_3O_7$ nanotube; 100 mL of 0.5 mM solution of Cu^{2+} [70]; 17.02 g Titanium n-butoxide; 0.8510 g silver nitrate [39]; 8.4 g (w/w = 10); 18.8 g (w/w = 20); 32.2 g (w/w = 30); 50.1 g (w/w = 40); 75.2 g (w/w = 50) [44]; 0.6 Mg/cm^2 [53]; 13.9 g/L [54]; 0.200 g of $AgNO_3$; 0.200 mL of CH_2Cl_2; 0.400 g α-Fe_2O [76]; 0.05 g [55]; and 0.0625 Mg/cm^2 [62]. There are various deposition techniques available to obtain nanostructured materials, including conventional and established methods, as well as emergent and alternative approaches. These methods involve coating directly on the surface or deposition of pre-synthesized nanostructured materials. The type of coating was not indicated in the works of Álvarez et al., 2022 [73], and Li et al., 2022 [75]. In the other works, the type of coating was: (i) method based on coating directly on the surface as a physical vapor deposition, including sputtering deposition [33,35,37,41,46,58,66,72] and spray coating [35,36,46,53,62,64,69]; (ii) deposition of pre-synthesized nanostructured materials, including dip coating [33,36,39,41,42,45,48,51,52,56,57,65,67,77], spin coating [34,44,47,71,76], drop coating [54,55,63,74], atmospheric pressure chemical vapor deposition (APCVD) [38,43,46], chemical process [50], manual coating [40], flame-assisted CVD (FACVD) [38], smearing [59,69], impregnation [59], pulsed-pressure metalorganic chemical vapor deposition (pp-MOCVD) [68], atomic layer deposition (ALD) [61], and multiple coating [60].

As shown in Table 2, 27 articles considered *Escherichia coli* as a microbial target [33–43,48–52,54–56,58,62,63,65,68,72,75,77], 16 *Staphylococcus aureus* [34,36,39,42,46,50,53,57–60,64,67,69,72,76], 4 *Pseudomonas aeruginosa* [34,42,71,75], 3 *Candida albicans* [55,61,72], 2 *Pseudomonas putida* [50,59], 2 *Aspergillus niger* [45,55], 2 *Listeria monocytogenes* [52,66], 2 *Staphylococcus epidermidis* [47,74], 1 *Legionella pneumophila* [70], 1 *MS2 virus* [36], 1 *Kocuria rhizophila* [45], 1 *Bacillus atrophaeus* [45], 1 *Bacillus cereus* [39], 1 *Salmonella typhimurium* [72], 1 *Bacillus anthracis* [52], 1 *Clostridium perfringens* [52], 1 *Listeria innocua* [50], and 1 Human coronavirus *229E* [73]. Bacteria can be classified in "Gram-positive" and "Gram-negative", based on the color they take on in Gram staining. This method uses crystal violet dye, which is retained by the thick peptidoglycan cell wall present in Gram-positive bacteria (20 to 80 nm, compared to 2–3 nm in Gram-negative bacteria). Therefore, this reaction gives these microorganisms a blue color [78]. Specifically, considering Gram strains, 21 articles of this systematic review considered Gram-positive bacteria (*S. aureus*, *L. monocytogenes*, *S. epidermidis*, *K. rhizophila*, *B. atrophaeus*, *B. cereus*, and *B. anthracis*), and 29 articles considered Gram-negative bacteria (*E. coli*, *P. aeruginosa*, *P. putida*, *L. pneumophila*, *S. typhimurium*, *C. perfringens*, and *L. innocua*). Also, two articles considered viruses (Human coronavirus *229E* and *MS2 virus*) and three articles fungi (*C. albicans* and *A. niger*). The physiology and microbial structure determine the photocatalytic inactivation efficiency. The structure of microorganisms is a crucial factor in determining their resistance to photocatalytic disinfection. Microorganisms have varying levels of resistance to photocatalytic disinfection. The order of disinfection susceptibility is as follows: molds, yeasts, Gram-positive bacteria, Gram-negative bacteria, and viruses [97]. Thus, in the case of viruses, relatively few outer structures are present, offering less resistance to inactivation by photocatalysis; for bacteria, Gram-positive bacteria have higher peptidoglycan content than Gram-negative bacteria and, for this reason, are more resistant [98–104]. The most widely used test for evaluation of antimicrobial activity was plate counting [33–36,38–41,43,45,46,48–51,53–58,60–63,66–72,74,76,77]; the other tests were: LIVE/DEAD Biofilm Viability Kit [37,52,59,64,65,69,75]; disk diffusion assay [47]; UV-induced bactericidal test [47]; qualitative Ag ion release in bacteria inoculated agar media [47]; surface topographical examination by laserscan profilometry [47]; endpoint titration method [73]; membrane integrity evaluation [71]; and cell attachment method [42].

Thirty-two articles considered UV as light source [33,35–47,49–52,54,59–62,64–71,75], 14 visible light [33,34,41,48,53,55–58,60,63,72,74,76,77], and one study used D65 (radiation that emulates daylight) [73]. The wavelength of the light varied from 254 [43,46,62] to 750 nm [73], and the distance of light source from the surface varied from 57 mm [46] to 30 cm [58].

Finally, the time of light exposition varied from 120 s [46] to 24 h [43,48,57,67,70]. In particular, nine studies considered 1 h of exposition [34,42,44,49–51,61,63,72]; seven studies 3 h [38,40,47,50,58,62,71]; five studies 2 h [52,53,55,59,69]; five studies 6 h [37,39,47,54,74]; five studies 24 h [43,48,57,67,70]; four studies 30 min [34,50,56,76]; four studies 90 min [34,36,41,42]; three studies 4 h [35,45,68]; three studies 20 min [42,50,66]; two studies 45 min [52,65]; one study 120 s [46]; one study 15 min [34]; one study 25 min [75]; one study 234 min [73]; one study 5 h [33]; one study 12 h [47]; and one study 18 h [64].

A meta-analysis was conducted based on 17 studies selected from 45 included in the systematic review (Table 3). In particular, 26 articles were excluded from the meta-analysis because they did not consider TiO_2 and 2 articles because they did not consider bacteria. For the meta-analysis, the bacteria considered in the included articles were grouped into Gram-positive (*L. monocytogenes*; *S. aureus*; *L. innocua;* and *K. rhizophila*) and Gram-negative (*E. coli*; *P. putida*; and *P. aeruginosa*). The surface types of the articles included in the meta-analysis were grouped into four groups (glass, ceramics, plastic, and steel); therefore, polypropylene [40], PVC [41], and polyethylene [62] were included in the "plastic" group. Coating types were also grouped: FACVD, APCVD [38], and ppMOCVD [68] were included in the "chemical process" group; smearing and impregnation [59] and sputtering deposition, APCVD, and spray [46] were included in the "multiple coating" group. Light sources were grouped according to nanometers into "UVA", "UVB", "UVC", "Visible", and "UV all" when not better specified. Finally, exposition time was also grouped into four groups: "2–30 min"; "31–90 min"; "91–180 min"; and ">180 min".

Table 3. Characteristics of the studies included in the meta-analysis.

Author, Year, Country	Gram Stain	Type of Surface	Type of Coating Method	Light Source	Time of Light Exposition	Microbial Reduction	Reference
Barthomeuf et al., 2019, France	Gram-positive	Glass	Sputtering deposition	UVA	2–30 min	99.5%	[66]
Bonetta et al., 2013, Italy	Gram-positive; Gram-negative	Ceramics	Chemical process	UVA	2–30 min; 31–90 min; 91–180 min	50%; 90%; 95%	[50]
Chawengkijwanich et al., 2008, Thailand	Gram-negative	Plastic	Manual coating	UVA	91–180 min	99.9%	[40]

Table 3. *Cont.*

Author, Year, Country	Gram Stain	Type of Surface	Type of Coating Method	Light Source	Time of Light Exposition	Microbial Reduction	Reference
Clemente et al., 2019, UK	Gram-positive	Glass	Dip coating	UVA	>180 min	100%	[67]
Evans et al., 2007, UK	Gram-negative	Steel	Chemical process	UV all	91–180 min	100%	[38]
Guo et al., 2013, China	Gram-negative	Glass	Dip coating	UV all	31–90 min	100%	[51]
Jalvo et al., 2017, Spain	Gram-positive; Gram-negative	Glass	Multiple coating	UVA; UVB	91–180 min	99.9%	[59]
Jalvo et al., 2018, Spain	Gram-positive	Glass	Spray coating	UV all	>180 min	99%	[64]
Krumdieck et al., 2019, New Zealand	Gram-negative	Steel	Chemical process	UVA	>180 min	99.9%	[68]
Lin et al., 2008, China	Gram-negative	Plastic	Dip coating	UVA	31–90 min	100%	[41]
Muranyi et al., 2010, Germany	Gram-positive	Glass	Dip coating	UVA	>180 min	99.9%	[45]
Nandakumar et al., 2017, USA	Gram-positive	Ceramics	Multiple coating	UVA; Visible	>180 min	45%	[60]
Pezzoni et al., 2020, Argentina	Gram-negative	Glass	Spin coating	UVA	91–180 min	99.9%	[71]
Shieh et al., 2006, Taiwan	Gram-negative	Glass; Steel	Sputtering deposition	UV all; Visible	>180 min	99.9%	[33]
Szczawiński et al., 2011, Poland	Gram-positive	Ceramics	Multiple coating	UVC	2–30 min	97%	[46]
Verdier et al., 2014, France	Gram-negative	Glass	Drop coating	UV all	>180 min	75%	[54]
Yemmireddy et al., 2017, USA	Gram-negative	Plastic	Spray coating	UVC	91–180 min	99.9%	[62]

3.3. Antimicrobial Efficacy of Coatings

After analyzing the results of the included studies, we have concluded that nanoparticle coating led to an increase in antimicrobial effectiveness. (Table 2). In the literature, different studies have assessed the variations in antimicrobial activity bases modified with TiO_2 nanoparticles. By analysis of pooled data, the TiO_2 coating had a strong explanatory force for the reduction of both Gram-positive and -negative bacteria strains (99.4%, Figure 3), and the subgroup analysis showed variations in removal efficiency for different surfaces (p = 0.005) and the time of exposure (p = 0.05) for Gram-positive strains. In particular, the glass surface was found to be the best in terms of antimicrobial efficacy, and the best time of light exposition was the one longer than 180 min (p = 0.001). Surface glass is mainly used in healthcare as bioactive glass [105]. In medicine and dentistry, it has several clinical applications involving hard tissue regeneration. In dentistry, photocatalysis has various applications, including dental restorative materials, mineralizing agents, coatings for dental implants, pulp capping, root canal treatment, and air abrasion. In medicine, photocatalysis has a wide range of applications, from orthopedics to soft tissue restoration [105]. Photocatalysis can also be used to inactivate harmful microbes, making it useful in various settings, such as medical, laboratory, industrial, and wastewater treatment [106,107]. UV light irradiation in the presence of a photocatalyst can be used to sterilize medical devices and body implants, such as dental implants. Photocatalyst coatings are commonly employed for this purpose [108]. TiO_2 films on chromium steel and titanium substrates allow for disinfection of implants that may be at risk of infection by bacteria such as *S. aureus* [108]. Furthermore, dressings used in medical treatment can be coated with polymer–metal nanocomposites to make them microbe-free. Photocatalysis is a great method also for preventing the spread of biological contaminants through the air, with implications for anthrax and other infectious contaminants [109].

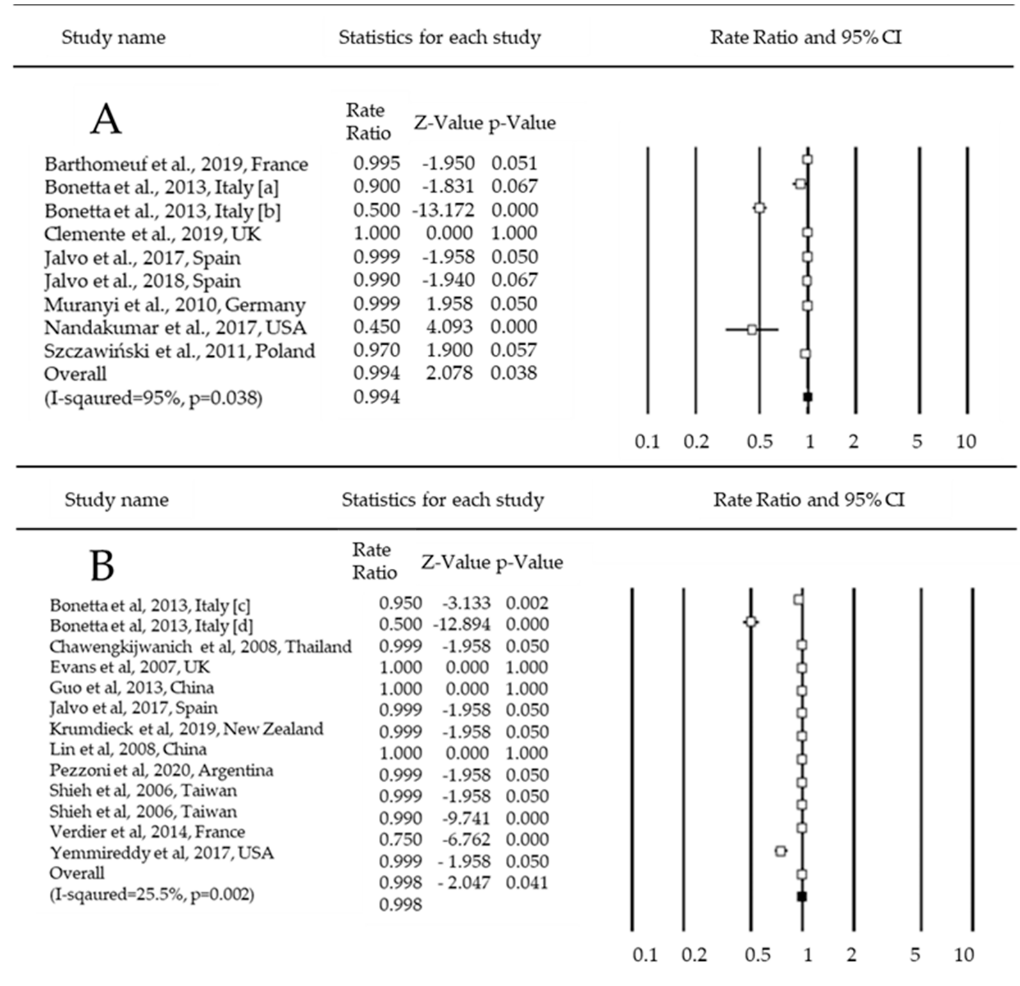

Figure 3. Forest plot. The bacterial reduction rate of coated-TiO_2, as indicated by the mean effect size and 95% confidence interval. (**A**) = Gram-positive; (**B**) = Gram-negative [33,38,40,41,45,46,50,51,54,59,60,62,64,66–68,71].

The meta-analysis showed that Gram-positive bacteria were more reduced than Gram-negative ones. This result is promising because Gram-positive bacteria are among the most widespread resistant pathogens, posing significant clinical challenges due to their immense genetic ability to acquire and develop resistance to antimicrobials. Gram-positive bacteria can generate spores that can survive in the environment [70,71,78,79]. These spores are one of the most resistant forms of life known to date and can tolerate various stresses, such as heat, chemicals, and harsh physical conditions [72,80]. The included meta-analysis articles are plotted in the forest plot below, and the bacteria strains are divided based on their classification (A = Gram-positive, and B = Gram-negative). The mechanism of TiO_2 toxicity towards microorganisms depends on the rupture of the cytoplasmic membrane and subsequent leakage of intracellular components [110,111]. Thus, hydroxyl radicals produced on the coating attack the cytoplasmic membrane, and the different morphologies of the outer layers of different Gram-positive and -negative bacteria hinder hydroxyl radical attack in different ways. The Gram-positive bacterium *S. aureus*, for example, has little protection from radicals, having only a periplasmic space and a peptidoglycan layer that, although thick, is composed of a rather open polymeric network of polysaccharide chains of N-acetylmuramic acid and N-acetylglucosamine with peptide bridges. The Gram-negative bacterium *E. coli*, on the other hand, has a layer of peptidoglycan in addition to an outer membrane composed of lipids, lipopolysaccharides, and proteins. This logic would explain the greater antimicrobial activity of Ag-TiO_2 against Gram-positive bacteria. Cell death occurs when the membrane is disrupted because there are no other barriers, such as TiO_2 [110,112].

The Q value for the influencing factors was very high (Q = 202.8, p = 0.001), showing that the type of the surface and process of coating can modulate bacterial removal efficiency and are influenced by each other. The study suggests that the interactions between different factors affecting bacterial removal in coatings should be further explored. Among the surface types, dip coating is the most effective (R = 0.0005, and p = 0.0001) in reducing bacteria, especially Gram-positive. Indeed, the dip coating method is one of the most widely used to deposit TiO_2 NPs. Among the principal proprieties, there are simplicity, reliability, reproducibility, and cost-effectiveness [113]. Dip coating has several advantages, such as being suitable to cover surfaces with different geometries, enabling coating of both sides of a substrate at once, and deposition is suitable for application in largescale processes [114]. Furthermore, dip coating methods can be used to coat a wide range of substrates, including metallic, ceramic, and polymeric surfaces, among others [115]. Similarly, spray coating is a commonly used deposition technique for applying TiO_2 NPs-based coatings on large surfaces due to its mild operating conditions and cost-effectiveness [113–115]. The superior wear resistance of TiO_2 nanoparticle coating may contribute to its antimicrobial effect [81,82]. Furthermore, even if surface defects appear after a certain number of times, the antifouling and antimicrobial properties can be maintained as long as the surface is surrounded by a significant coating of TiO_2 nanoparticles [83]. The future of this research field is focused on developing innovative photocatalytic and photo-electrocatalytic surfaces for microbial inactivation. These solutions should address gaps such as low utilization efficiency of sunlight [18–20] and the need for nanostructured photoanodes that can provide better electron transport and oxygen vacancy materials [116,117]. Additionally, synergic connection with other processes such as fuel cells or ozonation can improve disinfection performance [22].

3.4. Limitations of the Study

This systematic review and meta-analysis have limitations. Firstly, there is heterogeneity among the selected studies, with some not presenting an initial bacterial load, some failing to clarify the dose of photocatalyst used, and others lacking details on the wavelength, distance, and characteristics of the light source employed. Significant variations in the coating method exist, thereby restricting comparability and potentially undermining the consistency of the findings. This systematic review and meta-analysis mark the first endeavor to establish the antimicrobial efficacy of various photocatalysts adhered to distinct surfaces employing diverse coating techniques [23–26]. This initiates new possibilities for forthcoming research that can identify the most effective coating method for disinfecting pathogenic microorganisms that pose a danger to human health.

4. Conclusions

Microbial-based diseases and their spread remain a significant burden on the healthcare systems and economies of countries worldwide. Moreover, over the decades, microorganisms generated resistance against existing drugs due to misuse or overuse. To address these life-threatening problems, new alternatives have been sought. Antimicrobial photocatalyst-based materials have emerged as a tool to fight against pathogens, as highlighted in this review. These materials have been used as surface coatings to destroy

SARS-CoV-2. Antibacterial activity due to photocatalysis works by disrupting the cell envelope of bacteria. This means that the likelihood of pathogens developing resistance against photocatalysts is low or null, unlike conventional antibiotics that target specific areas. The goal is to develop antimicrobial coatings that are safe and can be used as an alternative to current antibiotics or disinfectants. This systematic review and meta-analysis work lays a promising foundation for this. Indeed, it was found that coating surfaces with photocatalysts has excellent disinfectant properties regardless of the type of coating, and it is effective on various microorganisms, even very resistant ones. The best surface is the glass, and the dip coating seems to be the better technology for the deposition of TiO_2. Moving forward, it is essential to include multi-drug-resistant and clinically isolated pathogens in research and development efforts. Moreover, proposals for developing novel materials that combine electrospinning and advanced oxidation technologies can be made. This can include synthetic strategies that take advantage of the unique properties of polymers and overcome the limits of current photocatalysts.

Author Contributions: Conceptualization, F.U. and F.V.; methodology, F.U., F.V., G.L. and V.V.; software, F.U., F.V. and V.V.; formal analysis, F.U., F.V., G.L. and V.V.; investigation, F.U., F.V., G.L. and V.V.; data curation, F.U., F.V. and V.V.; writing—original draft preparation, F.U. and F.V.; writing—review and editing, F.U., F.V. and G.L.; supervision F.V. and V.R.S. All authors have read and agreed to the published version of the manuscript.

Funding: This study was partially funded by the MIUR-Fund-PON R&I 2014–2020 React-EU and IUSM Projects (CUP H83C23000160001; Prot. 1007-2023).

Institutional Review Board Statement: Not applicable.

Informed Consent Statement: Not applicable.

Data Availability Statement: Not applicable.

Acknowledgments: The authors thank Manuela Camerino and Tiziana Zilli for library assistance.

Conflicts of Interest: The authors declare no conflicts of interest.

References

1. Wilson, A.M.; Weir, M.H.; King, M.F.; Jones, R.M. Comparing approaches for modelling indirect contact transmission of infectious diseases. *J. R. Soc. Interface* **2021**, *18*, 20210281. [CrossRef]
2. Atkinson, M.P.; Wein, L.M. Quantifying the routes of transmission for pandemic influenza. *Bull. Math. Biol.* **2008**, *70*, 820–867. [CrossRef]
3. Reed, S.E. An investigation of the possible transmission of rhinovirus colds through indirect contact. *J. Hyg.* **1975**, *75*, 249–258. [CrossRef] [PubMed]
4. Mubareka, S.; Lowen, A.C.; Steel, J.; Coates, A.L.; Carcia-Sastre, A.; Palese, P. Transmission of influenza virus via aerosols and fomites in the guinea pig model. *J. Infect. Dis.* **2009**, *199*, 858–865. [CrossRef] [PubMed]
5. Walther, B.A.; Ewald, P.W. Pathogen survival in the external environment and the evolution of virulence. *Biol. Rev.* **2004**, *79*, 849–869. [CrossRef]
6. Sze-To, G.N.; Yang, Y.; Kwan, J.K.; Yu, S.C.; Chao, C.Y. Effects of surface material, ventilation, and human behavior on indirect contact transmission risk of respiratory infection. *Risk. Anal.* **2014**, *34*, 818–830. [CrossRef]
7. Tuson, H.H.; Weibel, D.B. Bacteria–surface interactions. *Soft. Matter.* **2013**, *9*, 4368. [CrossRef] [PubMed]
8. Dancer, S.J. Controlling hospital-acquired infection: Focus on the role of the environment and new technologies for decontamination. *Clin. Microbiol. Rev.* **2014**, *27*, 665–690. [CrossRef]
9. Kumar, A.; Alam, A.; Rani, M.; Ehtesham, N.Z.; Hasnain, S.E. Biofilms: Survival and defense strategy for pathogens. *Int. J. Med. Microbiol.* **2017**, *307*, 481–489. [CrossRef]
10. Maillard, J.Y.; Centeleghe, I. How biofilm changes our understanding of cleaning and disinfection. *Antimicrob. Resist. Infect. Control.* **2023**, *12*, 95. [CrossRef]
11. Krukiewicz, K.; Kazek-Kęsik, A.; Brzychczy-Włoch, M.; Łos, M.J.; Ateba, C.N.; Mehrbod, P.; Ghavami, S.; Shyntum, D.Y. Recent Advances in the Control of Clinically Important Biofilms. *Int. J. Mol. Sci.* **2022**, *23*, 9526. [CrossRef] [PubMed]
12. Protano, C.; Cammalleri, V.; Romano Spica, V.; Valeriani, F.; Vitali, M. Hospital environment as a reservoir for cross transmission: Cleaning and disinfection procedures. *Ann. Ig.* **2019**, *31*, 436–448.
13. Cloutier, M.; Mantovani, D.; Rosei, F. Antibacterial Coatings: Challenges, Perspectives, and Opportunities. *Trends Biotechnol.* **2015**, *33*, 637–652. [CrossRef] [PubMed]

14. Banu, R.; Salvi, N.; Gupta, S.; Ameta, C.; Ameta, R.; Punjabi, P.B. A facile synthesis of GO/CuO nanocomposite with enhancing photocatalytic activity for the degradation of azure-B dye and its antimicrobial behavior. *Arab. J. Sci. Eng.* **2021**, *47*, 365–378. [CrossRef]
15. Kong, X.; Liu, X.; Zheng, Y.; Chu, P.K.; Zhang, Y.; Wu, S. Graphitic carbon nitride-based materials for photocatalytic antibacterial application. *Mater. Sci. Eng. R.* **2021**, *145*, 100610. [CrossRef]
16. Atacan, K.; Güy, N.; Özacar, M. Recent advances in photocatalytic coatings for antimicrobial surfaces. *Curr. Opin. Chem. Eng.* **2022**, *36*, 100777. [CrossRef]
17. Ganguly, P.; Byrne, C.; Breen, A.; Pillai, S.C. Antimicrobial activity of photocatalysts: Fundamentals, mechanisms, kinetics and recent advances. *Appl. Catal. B* **2018**, *225*, 51–75. [CrossRef]
18. Shahsavandi, F.; Amirjani, A.; Hosseini, H.R.M. Plasmon-enhanced photocatalytic activity in the visible range using AgNPs/polydopamine/graphitic carbon nitride nanocomposite. *Appl. Surf. Sci.* **2022**, *585*, 152728. [CrossRef]
19. Amirjani, A.; Amlashi, N.B.; Ahmadiani, Z.R. Plasmon-Enhanced Photocatalysis Based on Plasmonic Nanoparticles for Energy and Environmental Solutions: A Review. *ACS Appl. Nano Mater.* **2023**, *6*, 9085–9123. [CrossRef]
20. Liu, L.; Shen, Z.; Wang, C. Highly efficient visible-light-driven photocatalytic disinfection of flowing bioaerosol using mono/multilayer MXene based catalyst. *Chem. Eng. J.* **2023**, *457*, 141327. [CrossRef]
21. Zhang, P.; Lin, L.; Zang, D.; Guo, X.; Liu, M. Designing bioinspired anti-biofouling surfaces based on a superwettability strategy. *Small* **2017**, *13*, 1503334. [CrossRef] [PubMed]
22. Valenzuela, L.; Faraldos, M.; Bahamonde, A.; Rosal, R. Critical review on the use of photocatalysis and photoelectrocatalysis to create antimicrobial surfaces. *Curr. Opin. Chem. Eng.* **2021**, *34*, 100762. [CrossRef]
23. Schutte-Smith, M.; Erasmus, E.; Mogale, R.; Marogoa, N.; Jayiya, A.; Visser, H.G. Using visible light to activate antiviral and antimicrobial properties of TiO_2 nanoparticles in paints and coatings: Focus on new developments for frequent-touch surfaces in hospitals. *J. Coat. Technol. Res.* **2023**, *20*, 789–817. [CrossRef]
24. Rabajczyk, A.; Zielecka, M.; Klapsa, W.; Dziechciarz, A. Self-Cleaning Coatings and Surfaces of Modern Building Materials for the Removal of Some Air Pollutants. *Materials* **2021**, *14*, 2161. [CrossRef] [PubMed]
25. Margarucci, L.M.; Romano Spica, V.; Protano, C.; Gianfranceschi, G.; Giuliano, M.; Di Onofrio, V.; Mucci, N.; Valeriani, F.; Vitali, M.; Romano, F. Potential antimicrobial effects of photocatalytic nanothecnologies in hospital settings. *Ann. Ig.* **2019**, *31*, 461–473. [PubMed]
26. Byrne, J.A.; Dunlop, P.S.; Hamilton, J.W.; Fernández-Ibáñez, P.; Polo-López, I.; Sharma, P.K.; Vennard, A.S. A review of heterogeneous photocatalysis for water and surface disinfection. *Molecules* **2015**, *20*, 5574–5615. [CrossRef] [PubMed]
27. Page, M.J.; McKenzie, J.E. The PRISMA 2020 statement: An updated guideline for reporting systematic reviews. *BMJ* **2021**, *372*, 71. [CrossRef]
28. Covidence-Better Systematic Review Management. Available online: https://www.covidence.org/ (accessed on 31 July 2023).
29. Bender, R.; Friede, T.; Koch, A.; Kuss, O.; Schlattmann, P.; Schwarzer, G.; Skipka, G. Methods for evidence synthesis in the case of very few studies. *Res. Synth. Methods* **2018**, *9*, 382–392. [CrossRef] [PubMed]
30. Santabárbara, J.; Olaya, B.; Bueno-Notivol, J.; Pérez-Moreno, M.; Gracia-García, P.; Ozamiz-Etxebarria, N.; Idoiaga-Mondragon, N. Prevalence of depression among medical students during the COVID-19 pandemic. A systematic review and meta-analysis. *Rev. Med. Chil* **2021**, *149*, 1579–1588. [CrossRef] [PubMed]
31. Santabárbara, J.; Ozamiz-Etxebarria, N.; Idoiaga, N.; Olaya, B.; Bueno-Novitol, J. Meta-Analysis of Prevalence of Depression in Dental Students during COVID-19 Pandemic. *Medicina* **2021**, *57*, 1278. [CrossRef]
32. Oldenkamp, R.; Schultsz, C.; Mancini, E.; Cappuccio, A. Filling the gaps in the global prevalence map of clinical antimicrobial resistance. *Proc. Natl. Acad. Sci. USA* **2021**, *118*, e2013515118. [CrossRef]
33. Shieh, K.J.; Li, M.; Lee, Y.H.; Sheu, S.D.; Liu, Y.T.; Wang, Y.C. Antibacterial performance of photocatalyst thin film fabricated by defection effect in visible light. *Nanomedicine* **2006**, *2*, 121–126. [CrossRef] [PubMed]
34. Bletsa, E.; Merkl, P.; Thersleff, T.; Normark, S.; Henriques-Normark, B.; Sotiriou, G.A. Highly durable photocatalytic titanium suboxide–polymer nanocomposite films with visible light-triggered antibiofilm activity. *Chem. Eng. J.* **2023**, *454*, 139971. [CrossRef]
35. Cuadra, J.G.; Molina-Prados, S.; Mínguez-Vega, G. Multifunctional silver-coated transparent TiO_2 thin films for photocatalytic and antimicrobial applications. *Appl. Surf. Sci.* **2023**, *617*, 156519. [CrossRef]
36. Fu, H.; Yaniv, V.; Betzalel, Y.; Mamane, H.; Gray, K.A. Creating anti-viral high-touch surfaces using photocatalytic transparent films. *Chemosphere* **2023**, *323*, 138280. [CrossRef]
37. Todorova, N.; Minev, N.; Marinova, V.; Buchkov, K.; Videva, V.; Todorov, R.; Rafailov, P.; Strijkova, V.; Psycharis, V.; Giannakopoulou, T.; et al. Two-dimensional $PtSe_2$ coatings with antibacterial activity. *Appl. Surf. Sci.* **2023**, *611*, 155534. [CrossRef]
38. Evans, P.; Sheel, D.W. Photoactive and antibacterial TiO_2 thin films on stainless steel. *Surf. Coat. Technol.* **2007**, *201*, 9319–9324. [CrossRef]
39. Page, K.; Palgrave, R.G.; Parkin, I.P.; Wilson, M.; Savin, S.L.; Chadwick, A.V. Titania and silver–titania composite films on glass—Potent antimicrobial coatings. *J. Mater. Chem.* **2007**, *17*, 95–104. [CrossRef]
40. Chawengkijwanich, C.; Hayata, Y. Development of TiO_2 powder-coated food packaging film and its ability to inactivate Escherichia coli in vitro and in actual tests. *Int. J. Food. Microbiol.* **2008**, *123*, 288–292. [CrossRef]
41. Lin, H.; Xu, Z.; Wang, X.; Long, J.; Su, W.; Fu, X.; Lin, Q. Photocatalytic and antibacterial properties of medical-grade PVC material coated with TiO2 film. *J. Biomed. Mater. Res. B Appl. Biomater.* **2008**, *87*, 425–431. [CrossRef]

42. Yao, Y.; Ohko, Y.; Sekiguchi, Y.; Fujishima, A.; Kubota, Y. Self-sterilization using silicone catheters coated with Ag and TiO_2 nanocomposite thin film. *J. Biomed. Mater. Res. B Appl. Biomater.* **2008**, *85*, 453–460. [CrossRef] [PubMed]
43. Dunnill, C.W.H.; Aiken, Z.A.; Pratten, J. Enhanced photocatalytic activity under visible light in N-doped TiO_2 thin films produced by APCVD preparations using t-butylamine as a nitrogen source and their potential for antibacterial films. *J. Photochem. Photobiol. A Chem.* **2009**, *207*, 244–253. [CrossRef]
44. Sayilkan, F.; Asiltürk, M.; Kiraz, N.; Burunkaya, E.; Arpaç, E.; Sayilkan, H. Photocatalytic antibacterial performance of Sn^{4+}-doped TiO_2 thin films on glass substrate. *J. Hazard Mater.* **2009**, *162*, 1309–1316. [CrossRef] [PubMed]
45. Muranyi, P.; Schraml, C.; Wunderlich, J. Antimicrobial efficiency of titanium dioxide-coated surfaces. *J. Appl. Microbiol.* **2010**, *108*, 1966–1973. [CrossRef] [PubMed]
46. Szczawiński, J.; Tomaszewski, H.; Jackowska-Tracz, A.; Szczawińska, M.E. Survival of Staphylococcus aureus exposed to UV radiation on the surface of ceramic tiles coated with TiO_2. *Pol. J. Vet. Sci.* **2011**, *14*, 41–46. [CrossRef]
47. Akgun, B.A.; Wren, A.W.; Durucan, C.; Towler, M.R.; Mellott, N.P. Sol–gel derived silver-incorporated titania thin films on glass: Bactericidal and photocatalytic activity. *J. Sol.-Gel. Sci. Technol.* **2011**, *59*, 228–238. [CrossRef]
48. Chien, D.M.; Dung, D.T.M.; Dam, L.D. Preparation of nitrogen co-doped SiO_2/TiO_2 thin films on ceramic with enhanced photocatalytic activity under visible-light irradiation. *J. Exp. Nanosci.* **2012**, *7*, 254–262. [CrossRef]
49. Thongsuriwong, K.; Amornpitoksuk, P.; Suwanboon, S. Structure, morphology, photocatalytic and antibacterial activities of ZnO thin films prepared by sol–gel dip-coating method. *Adv. Powder Technol.* **2013**, *24*, 275–280. [CrossRef]
50. Bonetta, S.; Bonetta, S.; Motta, F.; Strini, A.; Carraro, E. Photocatalytic bacterial inactivation by TiO_2-coated surfaces. *AMB Express* **2013**, *3*, 59. [CrossRef]
51. Guo, M.Z.; Ling, T.C.; Poon, C.S. Nano-TiO_2-based architectural mortar for NO removal and bacteria inactivation: Influence of coating and weathering conditions. *Cem. Concr. Compos.* **2013**, *36*, 101–108. [CrossRef]
52. Roldán, M.V.; de Oña, P.; Castro, Y.; Durán, A.; Faccendini, P.; Lagier, C.; Grau, R.; Pellegri, N.S. Photocatalytic and biocidal activities of novel coating systems of mesoporous and dense TiO2-anatase containing silver nanoparticles. *Mater. Sci. Eng. C* **2014**, *43*, 630–640. [CrossRef] [PubMed]
53. Tallósy, S.P.; Janovák, L.; Ménesi, J. LED-light Activated Antibacterial Surfaces Using Silver-modified TiO_2 Embedded in Polymer Matrix. *J. Adv. Oxid. Technol.* **2014**, *17*, 9–16. [CrossRef]
54. Verdier, T.; Coutand, M.; Bertron, A.; Roques, C. Antibacterial Activity of TiO_2 Photocatalyst Alone or in Coatings on *E. coli*: The Influence of Methodological Aspects. *Coatings* **2014**, *4*, 670–686. [CrossRef]
55. Xiao, G.; Zhang, X.; Zhao, Y.; Su, H.; Tan, T. The behavior of active bactericidal and antifungal coating under visible light irradiation. *Appl. Surf. Sci.* **2014**, *292*, 756–763. [CrossRef]
56. Deng, W.; Ning, S.; Lin, Q.; Zhang, H.; Zhou, T.; Lin, H.; Long, J.; Lin, Q.; Wang, X. I-TiO_2/PVC film with highly photocatalytic antibacterial activity under visible light. *Colloids Surf. B Biointerfaces* **2016**, *144*, 196–202. [CrossRef]
57. Leyland, N.S.; Podporska-Carroll, J.; Browne, J.; Hinder, S.J.; Quilty, B.; Pillai, S.C. Highly Efficient F, Cu doped TiO_2 anti-bacterial visible light active photocatalytic coatings to combat hospital-acquired infections. *Sci. Rep.* **2016**, *6*, 24770. [CrossRef]
58. Chuang, K.T.; Abdullah, H.; Leu, S.J.; Cheng, K.B.; Kuo, D.H.; Chen, H.C.; Chien, J.H.; Hu, W.T. Metal oxide composite thin films made by magnetron sputtering for bactericidal application. *J. Photochem. Photobiol. A Chem.* **2017**, *337*, 151–164. [CrossRef]
59. Jalvo, B.; Faraldos, M.; Bahamonde, A.; Rosal, R. Antimicrobial and antibiofilm efficacy of self-cleaning surfaces functionalized by TiO_2 photocatalytic nanoparticles against Staphylococcus aureus and Pseudomonas putida. *J. Hazard. Mater.* **2017**, *340*, 160–170. [CrossRef]
60. Nandakumar, V.; Han, Z.; Fritz, Z.; Krishna, V.; Koopman, B.; Moudgil, B. Visible Light Photocatalytic Bacterial Inactivation on Titanium Dioxide Coatings. *KONA Powder Part. J.* **2017**, *34*, 234–240. [CrossRef]
61. Pessoa, R.S.; dos Santos, V.P.; Cardoso, S.B.; Doria, A.C.; Figueira, F.R.; Rodrigues, B.V.; Testoni, G.E.; Fraga, M.A.; Marciano, F.R.; Lobo, A.O.; et al. TiO_2 coatings via atomic layer deposition on polyurethane and polydimethylsiloxane substrates: Properties and effects on C. albicans growth and inactivation process. *Appl. Surf. Sci.* **2017**, *422*, 73–84. [CrossRef]
62. Yemmireddy, V.K.; Hung, Y.C. Photocatalytic TiO_2 coating of plastic cutting board to prevent microbial cross-contamination. *Food. Control* **2017**, *77*, 88–95. [CrossRef]
63. Hossain, M.A.; Elias, M.; Sarker, D.R.; Diba, Z.R.; Mithun, J.M.; Azad, M.A.; Siddiquey, I.A.; Rahman, M.M.; Uddin, J.; Uddin, M.N. Synthesis of Fe- or Ag-doped TiO2–MWCNT nanocomposite thin films and their visible-light-induced catalysis of dye degradation and antibacterial activity. *Res. Chem. Intermed.* **2018**, *44*, 2667–2683. [CrossRef]
64. Jalvo, B.; Faraldos, M.; Bahamonde, A.; Rosal, R. Antibacterial surfaces prepared by electrospray coating of photocatalytic nanoparticles. *Chem. Eng. J.* **2018**, *334*, 1108–1118. [CrossRef]
65. Won, Y.; Schwartzenberg, K.; Gray, K.A. TiO2-based transparent coatings create self-cleaning surfaces. *Chemosphere* **2018**, *208*, 899–906. [CrossRef] [PubMed]
66. Barthomeuf, M.; Castel, X.; Le Gendre, L.; Louis, J.; Denis, M.; Pissavin, C. Effect of Titanium Dioxide Film Thickness on Photocatalytic and Bactericidal Activities Against Listeria monocytogenes. *Photochem. Photobiol.* **2019**, *95*, 1035–1044. [CrossRef]

67. Clemente, A.; Ramsden, J.J.; Wright, A.; Iza, F.; Morrissey, J.A.; Li Puma, G.; Malik, D.J. Staphylococcus aureus resists UVA at low irradiance but succumbs in the presence of TiO2 photocatalytic coatings. *J. Photochem. Photobiol. B* **2019**, *193*, 131–139. [CrossRef]
68. Krumdieck, S.P.; Boichot, R.; Gorthy, R.; Land, J.G.; Lay, S.; Gardecka, A.J.; Polson, M.I.; Wasa, A.; Aitken, J.E.; Heinemann, J.A.; et al. Nanostructured TiO_2 anatase-rutile-carbon solid coating with visible light antimicrobial activity. *Sci. Rep.* **2019**, *9*, 1883. [CrossRef]
69. Valenzuela, L.; Iglesias, A.; Faraldos, M.; Bahamonde, A.; Rosal, R. Antimicrobial surfaces with self-cleaning properties functionalized by photocatalytic ZnO electrosprayed coatings. *J. Hazard. Mater.* **2019**, *369*, 665–673. [CrossRef]
70. Oder, M.; Koklič, T.; Umek, P.; Podlipec, R.; Štrancar, J.; Dobeic, M. Photocatalytic biocidal effect of copper doped TiO_2 nanotube coated surfaces under laminar flow, illuminated with UVA light on Legionella pneumophila. *PLoS ONE* **2020**, *15*, e0227574. [CrossRef]
71. Pezzoni, M.; Catalano, P.N.; Delgado, D.C.; Pizarro, R.A.; Bellino, M.G.; Costa, C.S. Antibiofilm effect of mesoporous titania coatings on Pseudomonas aeruginosa biofilms. *J. Photochem. Photobiol. B Biol.* **2020**, *203*, 111762. [CrossRef]
72. Zhao, Y.; Xu, J.; Li, Z.; Fu, T.; Jiang, S. In vitro antibacterial properties of $MoO_3/SiO_2/Ag_2O$ nanocomposite coating prepared by double cathode glow discharge technique. *Surf. Coat. Technol.* **2020**, *397*, 125992. [CrossRef]
73. Álvarez, Á.L.; Dalton, K.P.; Nicieza, I.; Abade Dos Santos, F.A.; de la Peña, P.; Domínguez, P.; Martin-Alonso, J.M.; Parra, F. Virucidal Properties of Photocatalytic Coating on Glass against a Model Human Coronavirus. *Microbiol. Spectr.* **2022**, *10*, e0026922. [CrossRef] [PubMed]
74. Du, J.; Li, Z.; Guo, H.; Zhu, E.; Liu, C.; Ren, B.; Che, G. The facile preparation and antibacterial performance of a conductive polymer-PU coating under visible light. *Prog. Org. Coat.* **2022**, *165*, 106755. [CrossRef]
75. Li, Y.; Liu, Y.; Yao, B.; Narasimalu, S.; Dong, Z. Rapid preparation and antimicrobial activity of polyurea coatings with RE-Doped nano-ZnO. *Microb. Biotechnol.* **2022**, *15*, 548–560. [CrossRef] [PubMed]
76. Vihodceva, S.; Šutka, A.; Otsus, M.; Vija, H.; Grase, L.; Kahru, A.; Kasemets, K. Visible-Light Active Flexible and Durable Photocatalytic Antibacterial Ethylene-co-vinyl Acetate—$Ag/AgCl/\alpha$-Fe_2O_3 Composite Coating. *Nanomaterials* **2022**, *12*, 1984. [CrossRef] [PubMed]
77. Xu, X.; Wang, Y.; Zhang, D.; Wang, J.; Yang, Z. In situ growth of photocatalytic Ag-decorated β-$Bi_2O_3/Bi_2O_{2.7}$ heterostructure film on PVC polymer matrices with self-cleaning and antibacterial properties. *Chem. Eng. J.* **2022**, *429*, 131058. [CrossRef]
78. Serrano-Aroca, Á.; Takayama, K.; Tuñón-Molina, A.; Seyran, M.; Hassan, S.S.; Pal Choudhury, P.; Uversky, V.N.; Lundstrom, K.; Adadi, P.; Palù, G.; et al. Carbon-based nanomaterials: Promising antiviral agents to combat COVID-19 in the microbial-resistant era. *ACS Nano* **2021**, *15*, 8069–8086. [CrossRef]
79. Chong, Y.; Ge, C.; Fang, G.; Wu, R.; Zhang, H.; Chai, Z.; Chen, C.; Yin, J.-J. Light-enhanced antibacterial activity of graphene oxide, mainly via accelerated electron transfer. *Environ. Sci. Technol.* **2017**, *51*, 10154–10161. [CrossRef]
80. Elias, L.; Taengua, R.; Frígols, B.; Salesa, B.; Serrano-Aroca, Á. Carbon nanomaterials and LED irradiation as antibacterial strategies against gram-positive multidrug-resistant pathogens. *Int. J. Mol. Sci.* **2019**, *20*, 3603. [CrossRef]
81. Endo-Kimura, M.; Kowalska, E. Plasmonic photocatalysts for microbiological applications. *Catalysts* **2020**, *10*, 824. [CrossRef]
82. Endo, M.; Wei, Z.S.; Wang, K.L.; Karabiyik, B.; Yoshiiri, K.; Rokicka, P.; Ohtani, B.; Markowska-Szczupak, A.; Kowalska, E. Noble metalmodified titania with visible-light activity for the decomposition of microorganisms. *Beilstein J. Nanotechnol.* **2018**, *9*, 829–841. [CrossRef] [PubMed]
83. Kowalska, E.; Wei, Z.; Karabiyik, B.; Herissan, A.; Janczarek, M.; Endo, M.; Markowska-Szczupak, A.; Remita, H.; Ohtani, B. Silvermodified titania with enhanced photocatalytic and antimicrobial properties under UV and visible light irradiation. *Catal. Today* **2015**, *252*, 136–142. [CrossRef]
84. Janczarek, M.; Endo-Kimura, M.; Wei, Z.; Bielan, Z.; Mogan, T.R.; Khedr, T.M.; Wang, K.; Markowska-Szczupak, A.; Kowalska, E. Novel structures and applications of graphene-based semiconductor photocatalysts: Faceted particles, photonic crystals, antimicrobial and magnetic properties. *Appl. Sci.* **2021**, *11*, 1982. [CrossRef]
85. Herrmann, J.M. Heterogeneous photocatalysis: State of the art and present applications. *Top. Catal.* **2005**, *34*, 49–65. [CrossRef]
86. Kong, D.B.; Ma, C.C.; Wang, W.; Liu, C.; Tian, Y.; Wang, T.; Zhao, Z.P.; Zhang, C.Y.; Feng, H.M.; Chen, S.G. Two birds with one stone: Interfacial controls and pH response for long-term and high efficiency Cu2O antibacterial materials. *Chem. Eng. J.* **2022**, *427*, 131734. [CrossRef]
87. Salvadores, F.; Reli, M.; Alfano, O.M.; Kocí, K.; Ballari, M.D. Efficiencies evaluation of photocatalytic paints under indoor and outdoor air conditions. *Front. Chem.* **2020**, *8*, 551710. [CrossRef]
88. Maulidiyah, M.; Susilowati, P.E.; Mudhafar, N.K.; Salim, L.A.; Wibowo, D.; Muzakkar, M.Z.; Irwan, I.; Arham, Z.; Nurdin, M. Photo-inactivation Staphylococcus aureus by using formulation of Mn-N-TiO_2 composite coated wall paint. *Biointerface Res. Appl. Chem.* **2022**, *12*, 1628–1637.
89. Abdulagatov, I.M.; Ragimov, R.M.; Khamidov, M.A.; Maksumova, A.M.; Abdullaeva, N.M. ALD coated polypropylene hernia meshes for prevention of mesh-related post-surgery complications: An experimental study in animals. *Biomed. Mater.* **2022**, *17*, 1. [CrossRef]
90. Ma, J.Z.; Liu, C.Y.; Yan, K. CQDs-MoS2 QDs loaded on Dendritic fibrous Nanosilica/Hydrophobic waterborne polyurethane acrylate for antibacterial coatings. *Chem. Eng. J.* **2022**, *429*, 132170. [CrossRef]

91. Tuñón-Molina, A.; Takayama, K.; Redwan, E.M.; Uversky, V.N.; Andrés, J.; Serrano-Aroca, Á. Protective face masks: Current status and future trends. *ACS Appl. Mater. Interfaces* **2021**, *13*, 56725–56751. [CrossRef]
92. Lu, Y.; Guan, S.; Hao, L.; Yoshida, H.; Nakada, S.; Takisawa, T.; Itoi, T. Inactivation of SARS-CoV-2 and photocatalytic degradation by TiO2 photocatalyst coatings. *Sci. Rep.* **2022**, *12*, 16038. [CrossRef] [PubMed]
93. Margarucci, L.M.; Gianfranceschi, G.; Romano Spica, V.; D'Ermo, G.; Refi, C.; Podico, M.; Vitali, M.; Romano, F.; Valeriani, F. Photocatalytic Treatments for Personal Protective Equipment: Experimental Microbiological Investigations and Perspectives for the Enhancement of Antimicrobial Activity by Micrometric TiO_2. *Int. J. Environ. Res. Public Health* **2021**, *18*, 8662. [CrossRef] [PubMed]
94. Guillard, C.; Lachheb, H.; Houas, A.; Ksibi, M.; Elaloui, E.; Herrmann, J.-M. Influence of chemical structure of dyes, of pH and of inorganic salts on their photocatalytic degradation by TiO_2 comparison of the efficiency of powder and supported TiO_2. *J. Photochem. Photobiol. A Chem.* **2003**, *158*, 27–36. [CrossRef]
95. Yang, Y.; Yan, Z.; Yang, S.; Tang, Z.; Li, W.; Yang, B.; Su, W.; Ji, T. Effect of substrate roughness on NOx removal of poly heptazine imides coated cement pastes exposed to washing and weathering. *J. Clean. Prod.* **2022**, *377*, 134397. [CrossRef]
96. Zhang, J.; Tan, H.; Deng, X. NOx removal ability of photocatalytic cement-based materials with porous structure. *J. Clean. Prod.* **2022**, *377*, 134396. [CrossRef]
97. Li, F.; Liu, G.; Liu, F.; Yang, S. A review of self-cleaning photocatalytic surface: Effect of surface characteristics on photocatalytic activity for NO. *Environ. Pollut.* **2023**, *327*, 121580. [CrossRef]
98. Ahlawat, K.; Jangra, R.; Ish, A.; Dixit, A.; Fulwani, D.; Jain, N.; Prakash, R. Analysis of a UV photocatalytic oxidation-based disinfection system for hydroxyl radicals, negative air ions generation and their impact on inactivation of pathogenic microorganisms. *Rev. Sci. Instrum.* **2023**, *94*, 104103. [CrossRef]
99. Sizar, O.; Leslie, S.W.; Unakal, C.G. Gram-Positive Bacteria. In *StatPearls [Internet]*; StatPearls Publishing: Treasure Island, FL, USA, 2023. Available online: https://www.ncbi.nlm.nih.gov/books/NBK470553/ (accessed on 31 December 2023).
100. Karaman, R.; Jubeh, B.; Breijyeh, Z. Resistance of Gram-Positive Bacteria to Current Antibacterial Agents and Overcoming Approaches. *Molecules* **2020**, *25*, 2888.
101. Wohlgemuth, S.; Kämpfer, P. BACTERIA | Bacterial Endospores. In *Encyclopedia of Food Microbiology*, 2nd ed.; Batt, C.A., Tortorello, M.L., Eds.; Academic Press: Cambridge, MA, USA, 2014; pp. 160–168.
102. Sawada, T.; Yoshino, F.; Kimoto, K.; Takahashi, Y.; Shibata, T.; Hamada, N.; Sawada, T.; Toyoda, M.; Lee, M.C. ESR detection of ROS Generated by TiO_2 coated with fluoridated apatite. *J. Dent. Res.* **2010**, *89*, 848–853. [CrossRef]
103. Kado, D.; Sakurai, K.; Sugiyama, T.; Ueda, T. Evaluation of cleanability of a titanium dioxide (TiO_2)-coated acrylic resin denture base. *Prosthodont. Res. Pract.* **2005**, *4*, 69–76. [CrossRef]
104. Alrahlah, A.; Fouad, H.; Hashem, M.; Niazy, A.A.; AlBadah, A. Titanium oxide (TiO_2)/polymethylmethacrylate (PMMA) denture base nanocomposites: Mechanical, viscoelastic and antibacterial behavior. *Materials* **2018**, *11*, 1096. [CrossRef] [PubMed]
105. Skallevold, H.E.; Rokaya, D.; Khurshid, Z.; Zafar, M.S. Bioactive Glass Applications in Dentistry. *Int. J. Mol. Sci.* **2019**, *20*, 5960. [CrossRef] [PubMed]
106. Khan, K.A.; Ghatak, H.R.; Ahuja, S.M. Photocatalytic technology: A review of environmental protection and renewable energy application for sustainable development. *Environ. Technol. Innov.* **2020**, *19*, 100893.
107. Ray, S.K.; Hur, J. A critical review on modulation of $NiMoO_4$-based materials for photocatalytic applications. *J. Environ. Manag.* **2021**, *278*, 111562. [CrossRef]
108. Kumaravel, V.; Nair, K.M.; Mathew, S.; Bartlett, J.; Kennedy, J.E.; Manning, H.G.; Whelan, B.J.; Leyland, N.S.; Pillai, S.C. Antimicrobial TiO_2 nanocomposite coatings for surfaces, dental and orthopaedic implants. *Chem. Eng. J.* **2021**, *416*, 129071. [CrossRef] [PubMed]
109. Rahimi, M.; Noruzi, E.; Sheyksaran, E.; Ebadi, B.; Kariminezhad, Z.; Molaparast, M.; Mehrabani, M.G.; Mehramouz, B.; Yousefi, M.; Ahmadi, R.; et al. Carbohydrate polymer-based silver nanocomposites: Recent progress in the antimicrobial wound dressings. *Carbohydr. Polym.* **2020**, *231*, 115696. [CrossRef]
110. Huang, Z.; Maness, P.C.; Blake, D.M.; Wolfrum, E.J.; Smolinski, S.L.; Jacoby, W.A. Bactericidal mode of titanium dioxide photocatalysis. *J. Photochem. Photobiol. A* **2000**, *130*, 163. [CrossRef]
111. Lu, Z.X.; Zhou, L.; Zhang, Z.L.; Shi, W.L.; Xie, Z.X.; Xie, H.Y.; Pang, D.W.; Shen, P. Cell Damage Induced by Photocatalysis of TiO_2 Thin Films. *Langmuir* **2003**, *19*, 8765. [CrossRef]
112. Sunada, K.; Watanabe, T.; Hashimoto, K. Studies on photokilling of bacteria on TiO_2 thin film. *J. Photochem. Photobiol. A* **2003**, *156*, 227. [CrossRef]
113. Dell'Edera, M.; Lo Porto, C.; De Pasquale, I.; Petronella, F.; Curri, M.L.; Agostiano, A.; Comparelli, R. Photocatalytic TiO_2-based coatings for environmental applications. *Catal. Today* **2021**, *380*, 62–83. [CrossRef]
114. Nabi, I.; Bacha, A.U.; Li, K.; Cheng, H.; Wang, T.; Liu, Y.; Ajmal, S.; Yang, Y.; Feng, Y.; Zhang, L. Complete Photocatalytic Mineralization of Microplastic on TiO_2 Nanoparticle Film. *IScience* **2020**, *23*, 101326. [CrossRef] [PubMed]
115. Kim, J.Y.; Youn, D.H. Nanomaterials for Advanced Photocatalytic Plastic Conversion. *Molecules* **2023**, *28*, 6502. [CrossRef] [PubMed]

116. Kouchehbaghi, N.H.; Sohrabi, M.; Razbin, M.; Daryakenari, A.A.; Abbasi, M.; Bahrami, S.A. Soft computing procedure to optimize the electrospinning parameters of polyacrylonitrile nanofibrous air filter. *J. Text. Inst.* **2023**. [CrossRef]
117. Lv, H.; Liu, Y.; Bai, Y.; Shi, H.; Zhou, W.; Chen, Y.; Liu, Y.; Yu, D.-G. Recent Combinations of Electrospinning with Photocatalytic Technology for Treating Polluted Water. *Catalysts* **2023**, *13*, 758. [CrossRef]